Statistical Properties of Wave Groups in a Random Sea State

Author(s): M. S. Longuet-Higgins

Source: *Philosophical Transactions of the Royal Society of London. Series A, Mathematical and Physical Sciences*, Oct. 12, 1984, Vol. 312, No. 1521, [Displayed chronologically; published out of order] (Oct. 12, 1984), pp. 219-250

Published by: Royal Society

Stable URL: https://www.jstor.org/stable/37397

Phil. Trans. R. Soc. Lond. A **312**, 219–250 (1984)
Printed in Great Britain

STATISTICAL PROPERTIES OF WAVE GROUPS IN A RANDOM SEA STATE

By M. S. LONGUET-HIGGINS, F.R.S.

Department of Applied Mathematics and Theoretical Physics, Silver Street, Cambridge CB3 9EW, U.K. and Institute of Oceanographic Sciences, Wormley, Godalming, Surrey GU8 5UB, U.K.

(*Received* 22 *November* 1983)

CONTENTS

Two apparently distinct approaches to the analysis of wave groups in a random sea state are described. In the first, the probabilities of the group-length G and the length of a 'high run' H are defined in terms of a wave envelope function $\rho(t)$. These lead naturally to expressions in terms of a single parameter ν that defines the spectral width.

In the second approach, the sequence of wave heights is treated as a Markov chain, with a non-zero correlation only between successive waves. This leads to expressions for G and H in terms of transition probabilities p_+ and p_-.

In this paper we find approximate analytic expressions for p_+ and p_- that show that the two approaches are roughly equivalent, to order ν.

Throughout the paper it is emphasized that the concept of a wave group assumes implicitly the neglect of those harmonic components that are either very short or very long compared with the peak frequency σ_p. That is, some filtering of the original record is implied. For typical records of wind waves it is found that a band-pass filter with upper and lower cut-offs at 1.5 σ_p and 0.5 σ_p is the most suitable.

 [Published 12 October 1984

Calculations are done for typical records of sea waves, and for some numerically simulated data, and there is agreement between the data and the analysis.

1. Introduction

A casual observer of the sea surface will notice that the heights of wind-generated waves are not uniform; they occur in successive groups of higher or lower waves; this leads to the popular but mistaken notion that 'every nth wave is the highest' where $n = 3$, 7 or 10, for example. In fact the wave groups are not all of equal length, as we shall see, but their group behaviour and other properties may be described with remarkable success by treating a typical record of the sea-surface elevation as a random Gaussian process, statistically steady in the short term, say over a duration of less than 30 min.

The Gaussian model, as applied to noise in electrical circuits, was first developed in well known papers by Rice (1944, 1958) and was applied to other aspects of sea waves by Longuet-Higgins (1952, 1957), Pierson (1962) and others. For a recent survey of the subject see Ochi (1982). The physical basis for the model is of course that the energy of surface waves at any point in the ocean arises from the action of wind in many different parts of the sea surface, in an essentially uncorrelated way. So long as linear superposition of the motions is valid, the surface displacements should therefore be Gaussian.

Particular attention to properties of *wave groups* in Gaussian noise was paid by Longuet-Higgins (1957, 1962) and Rice (1958). Recent interest in the subject (Goda 1970, 1983; Ewing 1973; Rye 1974; Kimura 1980 and others) has been stimulated by the suggestion that exceptional damage to ships, coastal defences or offshore structures may be caused by the occurrence of runs of successive high waves.

A further reason for interest in the subject is the relation of wave groups to the occurrence of wave breaking (see Donelan *et al.* 1972); also the probable effect of steep or breaking waves on the flow of air over the sea surface.

An essential preliminary to the analysis is to consider what we mean by a wave group, or indeed by a single wave, in a random sea. A typical observer counting high waves is not interested in the very short fluctuations, either ripples or short gravity waves, riding on the backs of the dominant waves. He does not include them in his count. Even if presented with an accurate instrumental record of the sea surface for analysis, he tends either to ignore the short waves or to smooth them out, for example by drawing a straight line between adjacent crests of the dominant waves, to represent the local wave height. Thus by paying attention at all to the group aspect of the wave record he is, consciously or otherwise, dealing with a filtered version of the wave record, from which the high frequencies have been eliminated or suppressed.

Similar considerations apply to the low frequency end of the spectrum. In analysing a record of a certain duration, say 20 min, we are not generally interested in the total mean surface level, but only in the crest-to-trough heights of the waves, or in the height of the crests relative to some local mean value, taken over a few waves only. Thus we subconsciously filter out those harmonic components of zero frequency or of frequency much lower than the dominant waves.

Part of our problem is then to arrive at a satisfactory method of filtering the record so as to retain only those aspects in which we are interested. This question is discussed in detail in §8.

The above point of view is implicit in the approach of Rice (1945, 1958), Longuet-Higgins (1957), and Nolte & Hsu (1972). These authors recognized that for a sufficiently narrow-band record a remarkably apt description of the group properties of a wave record can be given in terms of the wave-envelope function. For a Gaussian noise process, the envelope function can always be defined, even if the spectrum is not narrow; see §2. The statistics of the wave-envelope function $\rho(t)$ can be explored in much the same way as the statistics of the instantaneous surface elevation $\zeta(t)$. For example, the length of a wave group can be defined in terms of the number of times that the envelope $\rho(t)$ crosses a given reference level, say the 'significant' height of the waves. These statistics are all given in terms of the rth moments m_r of the spectral density function of $\zeta(t)$.

This classical approach has encountered some objections (Rye 1974) on the grounds that for typical spectra of wind-waves, the higher moments m_r, and in particular m_4, depend critically upon the high-frequency cut-off in the spectrum. But we have seen that the existence of such a cut-off, or filter, is really inherent in the phenomenon under discussion: the shorter the waves that we consider, then the shorter also must be the average group-length. Moreover, as we shall emphasize below, if the definitions of group-length suggested by Longuet-Higgins (1957) and by Nolte & Hsu (1972) are employed, then only the lower moment m_2 is involved, unlike Rice's (1945) definition, which depended on the maxima of ρ, hence the fourth moment m_4.

An alternative approach has been suggested by Sawnhey (1962), Wilson & Baird (1972), Kimura (1980) and others, namely to consider the correlation between successive, or almost successive, waves, without consideration of the frequency spectrum. Besides separating the model further from the physics, it should be clear that this approach by no means avoids the question of what filter is in fact applied to the wave record by an observer who selects, by some unstated criterion, the local wave height. None the less, the relation of this theory to the previous theory is of some interest.

The present paper falls into two parts. In §§2–9 we state and develop essentially the Rice, or envelope, theory, based on the spectral moments. Formulae are given for the average number of waves $\bar{G}$ in a group and for the mean number of waves $\bar{H}$ in a high run (see §§4 and 5 respectively). These are seen to depend only on the critical level $\rho = \rho^*$ and on the dimensionless bandwidth parameter

$$\nu^2 = m_2 m_0/m_1^2 - 1. \tag{1.1}$$

For swell, it appears that ν lies typically between 0.05 and 0.15. For wind waves, ν has a lower bound at about 0.35, before filtering. In §7 we discuss the calculation of the wave envelope (figures 1 *c–e*) and in §8 we show by applying this to typical wave records that the theoretical expressions for $\bar{G}$ and $\bar{H}$ agree well with the data (see for example figures 3–5). The frequency filter which gives results best in accord with visual measurements is found to be one having lower and upper cut-offs at 0.5 and 1.5 times the peak frequency.

In §9 we give a very rough theory for the probability density of G and H. Simple arguments suggest that for large G and H the densities $p(G)$ and $p(H)$ are both exponential, and this is supported by the available data. However the reasoning is not really applicable to smaller values of G and H.

Accordingly in the remainder of the paper we consider the alternative approach mentioned above, in which the wave heights are treated as a Markov chain, with a positive correlation γ only between successive waves. We derive an approximate relation between γ and ν, namely

$$\gamma \doteqdot 1 - 4\pi^2\nu^2, \tag{1.2}$$

which, however, is valid only for sufficiently small values of ν. It is shown in §11 that the effect of filtering can be to bring the spectral width to within the range of validity of (1.2). In §12 we give a simplified version of the Markov theory for $p(G)$ and $p(H)$ and show that filtering of the spectrum produces a perceptable improvement in the agreement between the theoretical distributions and Kimura's (1980) data (see figures 17–20).

Finally, by adopting further rough approximations to the Markov transition probabilities p_+ and p_- we show that the Rice (envelope) theory and the Markov chain theory are in remarkably good agreement, over a useful intermediate range of ν.

The main conclusions, together with further discussion, are restated in §13.

In an Appendix we derive the properties of an analytic expression for the spectral density function that may be of use in the description of ocean swell.

2. Definitions: the wave envelope

We assume that the surface elevation ζ may be represented as a stationary random function of the time t, with correlation function

$$\psi(\tau) = \overline{f(t)f(t+\tau)} \tag{2.1}$$

(a bar denoting the mean value with respect to t). The energy spectrum $E(\sigma)$ is related to $\psi(\tau)$ by

$$E(\sigma) = \frac{1}{\pi}\int_0^\infty \psi(\tau)\cos\sigma\tau\,\mathrm{d}\tau \tag{2.2}$$

and so

$$\psi(\tau) = \int_0^\infty E(\sigma)\cos\sigma\tau\,\mathrm{d}\sigma, \tag{2.3}$$

We assume also that over some finite time interval $(-\frac{1}{2}T, \frac{1}{2}T)$ the function ζ may be represented as a Fourier sum:

$$\zeta = \sum_{n=0}^{\infty} c_n \cos(\sigma_n t + \epsilon_n), \tag{2.4}$$

where $\sigma_n = 2n\pi/T$, the phases ϵ_n are distributed uniformly over $(0, 2\pi)$ and the amplitudes c_n are such that

$$\lim_{T\to\infty} \sum_{\mathrm{d}\sigma} \tfrac{1}{2}c_n^2 = E(\sigma)\,\mathrm{d}\sigma \tag{2.5}$$

to order $\mathrm{d}\sigma$, the summation being over any small but fixed frequency range $(\sigma, \sigma+\mathrm{d}\sigma)$.

The spectral moments m_r are defined by

$$m_r = \int_0^\infty \sigma^r E(\sigma)\,\mathrm{d}\sigma, \tag{2.6}$$

so that by (2.1)

$$m_0 = \int_0^\infty E(\sigma)\,\mathrm{d}\sigma = \psi(0) = \overline{\zeta^2} \tag{2.7}$$

represents the mean-square surface displacement and

$$\bar{\sigma} = m_1/m_0 \tag{2.8}$$

may be defined as the 'mean frequency'. If μ_r denotes the rth moment of $E(\sigma)$ about the mean, i.e.

$$\mu_r = \int_0^\infty (\sigma-\bar{\sigma})^r E(\sigma)\,\mathrm{d}\sigma, \tag{2.9}$$

then clearly

$$\mu_0 = m_0, \qquad \mu_1 = 0, \qquad \mu_2 = m_2 - m_1^2/m_0 \tag{2.10}$$

and we may define the spectral width parameter ν by

$$\nu^2 = \mu_2/\mu_0\,\bar{\sigma}^2 = m_2 m_0/m_1^2 - 1. \tag{2.11}$$

When $\nu^2 \ll 1$ we say that the spectrum is narrow.

Even when the spectrum is not necessarily narrow, it is possible to define the complex envelope function $A(t)$ by writing (2.4) in the form

$$\zeta = \operatorname{Re} A(t)\,\mathrm{e}^{\mathrm{i}\bar{\sigma}t}, \tag{2.12}$$

where

$$A = \sum_n c_n\,\mathrm{e}^{\mathrm{i}[(\sigma_n - \bar{\sigma})t + \epsilon_n]} = \rho \mathrm{e}^{\mathrm{i}\phi} \tag{2.13}$$

say. Here $\rho(t)$ may be called the real envelope function, or wave-amplitude, and $\phi(t)$ the phase. The real and imaginary parts of A are given by

$$\left.\begin{aligned} \rho\cos\phi &= \sum_n c_n \cos\,[(\sigma_n - \bar{\sigma})\,t + \epsilon_n], \\ \rho\sin\phi &= \sum_n c_n \sin\,[(\sigma_n - \bar{\sigma})\,t + \epsilon_n], \end{aligned}\right\} \tag{2.14}$$

and we shall see in §7 how these may always be computed, given only the initial function $\zeta(t)$.

From (2.13) it will be seen that the time derivative $\dot{A} = \mathrm{d}A/\mathrm{d}t$ contains, under the summation on the right, the factor $(\sigma_n - \bar{\sigma})$, so that

$$\overline{|\dot{A}|^2} = \mu_2 \tag{2.15}$$

and when the spectrum is narrow A varies slowly, on average, compared with the carrier wave $\mathrm{e}^{\mathrm{i}\bar{\sigma}t}$. Thus the wave record is practically sinusoidal, and the local, crest-to-trough, wave height is given by 2ρ, very nearly. A closer inspection suggests that the assumption is correct at least to order ν. Some terms of order ν^2 will nevertheless be carried along in the analysis.

3. Preliminary results

We begin by stating some known exact results of which proofs may be found, for example, in the papers by Rice (1944–1945, 1958) or Longuet-Higgins (1957).

The probability density (or simply 'density') of the function ζ is Gaussian:

$$p(\zeta) = (2\pi m_0)^{-\frac{1}{2}}\,\mathrm{e}^{-\zeta^2/2m_0}; \tag{3.1}$$

and similarly for the derivative $\dot{\zeta}$ of ζ:

$$p(\dot{\zeta}) = (2\pi m_2)^{-\frac{1}{2}}\,\mathrm{e}^{-\dot{\zeta}^2/2m_2}. \tag{3.2}$$

The joint density of ζ and $\dot{\zeta}$ satisfies

$$p(\zeta, \dot{\zeta}) = p(\zeta)\,p(\dot{\zeta}), \tag{3.3}$$

so that ζ and $\dot{\zeta}$ are statistically independent. The number of up-crossings by ζ of a given level ζ per unit time, is given by

$$N = \int_0^\infty p(\zeta, \dot{\zeta})\,\dot{\zeta}\,\mathrm{d}\dot{\zeta} = (2\pi)^{-\frac{1}{2}}\,(m_2/m_0)^{\frac{1}{2}}\,\mathrm{e}^{-\zeta^2/2m_0}. \tag{3.4}$$

This number is a maximum at the mean level $\zeta = 0$, so

$$N_{\max} = (2\pi)^{-\frac{1}{2}}(m_2/m_0)^{\frac{1}{2}}. \tag{3.5}$$

Corresponding results for the wave envelope ρ are as follows:

$$p(\rho) = (\rho/\mu_0)\,\mathrm{e}^{-\rho^2/2\mu_0}, \tag{3.6}$$

and

$$p(\dot\rho) = (2\pi\mu_2)^{-\frac{1}{2}}\,\mathrm{e}^{-\dot\rho^2/2\mu_2}, \tag{3.7}$$

(i.e. the densities of ρ and $\dot\rho$ are Rayleigh and Gaussian respectively), and

$$p(\rho,\dot\rho) = p(\rho)\,p(\dot\rho) \tag{3.8}$$

as in (3.3). The number of up-crossings of a given level per unit time by the wave envelope is

$$N' = \int_0^\infty p(\rho,\dot\rho)\,\dot\rho\,\mathrm{d}\dot\rho = (\mu_2/2\pi)^{\frac{1}{2}}p(\rho). \tag{3.9}$$

This number is a maximum when $p(\rho)$ is a maximum, i.e. when $\rho = \mu_0^{\frac{1}{2}}$, hence

$$N'_{\max} = (2\pi\mathrm{e})^{-\frac{1}{2}}(\mu_2/\mu_0)^{\frac{1}{2}}. \tag{3.10}$$

4. The average group length

In defining a group of high waves, we might consider the statistics of the *maxima* of the wave envelope. However, the mean number of maxima of $\rho(t)$, given by

$$\int_{-\infty}^0 p(\dot\rho,\ddot\rho)_{\dot\rho=0}\,|\ddot\rho|\,\mathrm{d}\ddot\rho, \tag{4.1}$$

involves the joint density $p(\dot\rho,\ddot\rho)$, which depends on the fourth moment μ_4, hence m_4 (see Rice 1945). In addition, we are not really interested in small fluctuations of the wave height, but only in broader features of the group.

We therefore adopt a lower-order definition of the length l of a wave group as the time interval between two successive upcrossings of some chosen level ρ; see Longuet-Higgins 1957; Ewing 1973. The mean length of wave groups, so defined, is then

$$\bar l = 1/N', \tag{4.2}$$

where $N'(\rho)$ is given by (3.9). Clearly $\bar l$ depends upon the arbitrary chosen level ρ. However there is one particular level for which N' is a maximum. At this level $\bar l$ is stationary with respect to small variations in ρ. Such a level may be particularly useful for determining $\bar l$ empirically, since the value of $\bar l$ so determined will be insensitive to small errors in the chosen level. From (3.6) this level occurs precisely when $\rho/\mu_0^{\frac{1}{2}} = 1$, giving

$$\bar l_{\min} = (2\pi\mathrm{e})^{\frac{1}{2}}(\mu_0/\mu_2)^{\frac{1}{2}}. \tag{4.3}$$

Since for a narrow spectrum the wavelength is almost constant at $1/N_{\max}$, where $N_{\max}$ is given by (3.5), the mean number of waves in a group, in general, is

$$\bar G = \bar l N_{\max} = (2\pi)^{-\frac{1}{2}}(m_2/\mu_2)^{\frac{1}{2}}(\mu_0^{\frac{1}{2}}/\rho)\,\mathrm{e}^{\rho^2/2\mu_0}. \tag{4.4}$$

Table 1. Values of $\bar{G}$ and $\bar{H}$ as functions of the spectral width parameter ν

		$\bar{G}$			$\bar{H}$	
ν	$\rho/\mu_0^{\frac{1}{2}}=1$	$(\frac{1}{2}\pi)^{\frac{1}{2}}$	2	1	$(\frac{1}{2}\pi)^{\frac{1}{2}}$	2
0.05	13.2	14.0	29.5	8.0	6.4	4.0
0.06	11.0	11.7	24.6	6.7	5.3	3.3
0.08	8.2	8.8	18.5	5.0	4.0	2.5
0.10	6.6	7.0	14.8	4.0	3.2	2.0
0.12	5.5	5.9	12.4	3.3	2.7	1.7
0.15	4.4	4.7	9.9	2.7	2.1	1.3
0.20	3.4	3.6	7.5	2.0	1.6	1.0
0.25	2.7	2.9	6.1	1.6	1.3	0.8
0.30	2.3	2.4	5.1	1.4	1.1	0.7
0.35	2.0	2.1	4.5	1.2	1.0	0.6

In terms of the parameter ν this is

$$\bar{G} = (2\pi)^{-\frac{1}{2}}\,[(1+\nu^2)^{\frac{1}{2}}/\nu]\,(\mu_0^{\frac{1}{2}}/\rho)\,\mathrm{e}^{\rho^2/2\mu_0}, \tag{4.5}$$

which is inversely proportional to ν, when ν is small. The minimum group length is when $\rho/\mu_0^{\frac{1}{2}} = 1$, so

$$\bar{G}_{\min} = (\mathrm{e}/2\pi)^{\frac{1}{2}}\,(1+\nu^2)^{\frac{1}{2}}/\nu = 0.6577\,(1+\nu^2)^{\frac{1}{2}}/\nu. \tag{4.6}$$

The values of $\bar{G}_{\min}$ for some representative values of ν are shown in the second column of table 1. In the third column are shown the corresponding values of $\bar{G}$ when the critical value of ρ is taken as the mean wave amplitude $\rho = (\frac{1}{2}\pi)^{\frac{1}{2}}\mu_0^{\frac{1}{2}}$. In the fourth column are the values when $\rho = 2\mu_0^{\frac{1}{2}}$, which is close to the significant wave amplitude $\rho = 2.003\,\mu_0^{\frac{1}{2}}$. For these two columns, the numerical constant in (4.6) is replaced by 0.6981 and 1.4739 respectively.

5. Runs of high waves

Consider now a different quantity: the number of successive waves exceeding a specified level ρ. We denote this by $H(\rho)$.

To obtain an average value $H(\rho)$, Rice (1958) reasoned that from the known density (3.6) the proportion of time during which ρ exceeded the given level would be

$$q(\rho) = \int_\rho^\infty p(\rho)\,\mathrm{d}\rho = \mathrm{e}^{-\rho^2/2\mu_0}. \tag{5.1}$$

Hence the average length of a 'high run' would be

$$\bar{l}' = q\bar{l} = q/N'. \tag{5.2}$$

By (3.6) and (3.9) this is

$$\bar{l}' = (2\pi/\mu_2)^{\frac{1}{2}}\,\mu_0/\rho. \tag{5.3}$$

To estimate the average number $\bar{H}$ of waves in a high run we multiply $\bar{l}'$ by the mean up-crossing rate $N_{\max}$ (see equation (3.5)) to give

$$\bar{H} = (2\pi)^{-\frac{1}{2}}\,(m_2/\mu_2)^{\frac{1}{2}}\,\mu_0^{\frac{1}{2}}/\rho, \tag{5.4}$$

or in terms of ν

$$\bar{H} = (2\pi)^{-\frac{1}{2}}\,[(1+\nu^2)^{\frac{1}{2}}/\nu]\,\mu_0^{\frac{1}{2}}/\rho, \tag{5.5}$$

This varies very simply like ρ^{-1}. If we take the reference level as $\rho = \mu_0^{\frac{1}{2}}$, then

$$\bar{H} = 0.3989\,(1+\nu^2)^{\frac{1}{2}}/\nu. \tag{5.6}$$

On the other hand, at the mean level $\rho/\mu_0^{\frac{1}{2}} = (\frac{1}{2}\pi)^{\frac{1}{2}}$ or the significant wave amplitude $\rho/\mu_0^{\frac{1}{2}} \approx 2$ the numerical constant in (5.6) is replaced by 0.3183 or 0.1995 respectively.

Representative values for $\bar{H}$ are given in table 1. It will be observed that since

$$\bar{H}/\bar{G} < q < 1, \tag{5.7}$$

$\bar{H}$ is always less than $\bar{G}$.

6. Parameters for ocean waves

For ocean swell, values of ν equal to 0.15 or less may be typical, as we shall see below. A spectrum of pure swell is band-limited, so that as a very simple model it is fair to assume

$$E(\sigma) = \begin{cases} \alpha, & |\sigma-\bar{\sigma}| < \delta\bar{\sigma}, \\ 0, & |\sigma-\bar{\sigma}| > \delta\bar{\sigma}, \end{cases} \tag{6.1}$$

where $\delta \leqslant 0.5$ say. For such a spectrum we have

$$\nu = \delta/\surd 3 \leqslant 0.289. \tag{6.2}$$

A convenient expression for an ocean swell spectrum having a smooth cut-off is

$$E(\sigma) = \alpha\sigma^{-\frac{1}{2}}\,\mathrm{e}^{-\frac{1}{2}n[\beta\sigma+(\beta\sigma)^{-1}]}, \tag{6.3}$$

where α, β and n are constants. For such a spectrum it may be shown (see the Appendix) that

$$\left.\begin{aligned} m_0 &= 2\alpha(\pi/\beta)^{\frac{1}{2}}/n\mathrm{e}^n, \\ \bar{\sigma} &= (1+1/n)/\beta, \\ \nu &= (n+2)^{\frac{1}{2}}/(n+1). \end{aligned}\right\} \tag{6.4}$$

When n is large we have $\nu \sim n^{-\frac{1}{2}}$. Hence useful values of n will lie in the range 50 to 500. We note that the spectrum (5.3) has a half-width $\beta\delta'$ given approximately by

$$\beta\sigma + (\beta\sigma)^{-1} = 2\ln 2, \tag{6.5}$$

hence

$$\delta' \sim (\ln 4)^{\frac{1}{2}}/n + O(n^{-\frac{3}{2}}), \tag{6.6}$$

corresponding to

$$\nu \sim n^{\frac{1}{2}} \sim 0.849\,\delta', \tag{6.7}$$

as compared with

$$\nu = \delta/\surd 3 = 0.577\,\delta \tag{6.8}$$

for the simple band-pass spectrum. The rule (6.7) should be fairly easy to apply in practice.

On the other hand for wind-waves, a typical form is the Pierson–Moskowitz spectrum

$$E(\sigma) = \alpha\sigma^{-5}\,\mathrm{e}^{-(\beta/\sigma)^\gamma} \tag{6.9}$$

where α, β and γ are constants depending on the wave field. It is easily shown that the rth moment m_r is given by

$$m_r = (\alpha\beta^{r-4}/\gamma)\,\Gamma((4-r)/\gamma), \tag{6.10}$$

where $\Gamma(z)$ is the usual gamma function: $\Gamma(n) = (n-1)!$ Hence we have

$$\bar{\sigma} = \beta\,\Gamma(3/\gamma)/\Gamma(4/\gamma) \tag{6.11}$$

independently of α, and

$$\nu^2 = \frac{\Gamma(2/\gamma)\,\Gamma(4/\gamma)}{[\Gamma(3/\gamma)]^2} - 1, \tag{6.12}$$

independently of both α and β. Some values of m_0, $\bar{\sigma}$ and ν are given in table 2. It can be seen that as γ decreases from ∞ to 1, so ν ranges from $8^{-\frac{1}{2}} = 0.3536$ to $2^{-\frac{1}{2}} = 0.7071$. The value $\gamma = \infty$ corresponds to the Phillips spectrum

$$E(\sigma) = \begin{cases} 0, & \sigma/\beta < 1, \\ \alpha\sigma^{-5}, & \sigma/\beta > 1. \end{cases} \tag{6.13}$$

A common value of γ is 4, when $\nu = 0.4247$.

Table 2. Parameters for the Pierson–Moskowitz spectrum (6.9)

γ	$m_0'\beta^4/\alpha$	$\bar{\sigma}'/\beta$	ν	ν'
∞	0.2500	1.3333	0.3536	0.1132
10	.2218	1.3487	.3713	.1314
8	.2216	1.3374	.3790	.1405
6	.2257	1.3089	.3933	.1570
5	.2328	1.2791	.4056	.1711
4	.2500	1.2254	.4247	.1804
3	.2977	1.1198	.4574	.1939
2	.5000	0.8862	.5227	.2151
1	6.0000	0.3333	.7071	.2483

However, we shall see later (§8) that for broad spectra, such as the Pierson–Moskowitz spectrum, it is implicit in the definition of a wave group that we use a filtered version of the spectrum, the T.P.M. or 'Truncated Pierson–Moskowitz' spectrum. This in general reduces the value of ν to a value ν' depending on the cut-off frequencies. Some values of ν' are given in the last column of table 2.

7. Calculation of the wave envelope

Records of sea waves are commonly in digital form, the surface elevation $\zeta(t)$ being specified at discrete but uniformly spaced times $t_1, t_2, \ldots t_M$ say. To calculate the wave envelope function

$$\rho = (\zeta^2 + \eta^2)^{\frac{1}{2}} \tag{7.1}$$

of §2, we need both the surface elevation $\zeta(t)$ itself and its Hilbert transform $\eta(t)$. For very long records it may be convenient to use a discrete form of the formula

$$\eta(t) = \frac{1}{\pi} ⨍_{-\infty}^{\infty} \frac{\zeta(s)}{t-s}\,\mathrm{d}s, \tag{7.2}$$

where $⨍$ denotes the principal value of the integral. For example, if $\zeta = \cos\sigma t$ then $\eta = \sin\sigma t$. However, for short or moderately long records, say $M \leqslant 10^4$, a method based on Fourier analysis is practical and more feasible.

Let ζ_m denote $\zeta(t_m)$, and set

$$\left.\begin{aligned} a_n &= \frac{1}{M}\sum_{m=1}^{M} \zeta_m \cos m\sigma_n, \\ b_n &= \frac{1}{M}\sum_{m=1}^{M} \zeta_m \sin m\sigma_n, \end{aligned}\right\} \tag{7.3}$$

where

$$\sigma_n = 2n\pi/M. \tag{7.4}$$

In particular,

$$a_M = \frac{1}{M}\sum_m \zeta_m, \qquad b_M = 0. \tag{7.5}$$

It is easy to show that

$$\zeta_m = \sum_{n=1}^{M} (a_n \cos m\sigma_n + b_n \sin m\sigma_n). \tag{7.6}$$

However, we shall dispense with the upper frequencies ($n > \frac{1}{2}M$) by using instead the identity

$$\zeta_m = 2\sum_{n=1}^{\frac{1}{2}M} (a_n \cos m\sigma_n + b_n \sin m\sigma_n) - (-1)^M a_{\frac{1}{2}M} + a_M \tag{7.7}$$

(M is assumed even). We may then take

$$\eta_m = 2\sum_{n=1}^{\frac{1}{2}M} (a_n \sin m\sigma_n - b_n \cos m\sigma_n). \tag{7.8}$$

In practice, the low-frequency component of the record is of no interest generally when considering crest-to-trough wave heights; for example, a non-zero mean value α_M is irrelevant. Hence in any examination of the properties of wave heights, or of the wave envelope, it is appropriate to work with a filtered version of the record and its transform:

$$\left.\begin{aligned} \zeta'_m &= 2\sum_{n'}^{n''} (a_n \cos m\sigma_n + b_n \sin m\sigma_n), \\ \eta'_m &= 2\sum_{n'}^{n''} (a_n \sin m\sigma_n - b_n \cos m\sigma_n), \end{aligned}\right\} \tag{7.9}$$

where n' and n'' are suitably chosen numbers such that $1 \leqslant n' < n'' < \frac{1}{2}M$. A reduction in the upper limit may be desirable to avoid the aliassing of energy from frequencies higher than the Nyquist frequency $\sigma_{\frac{1}{2}M}$.

We may then calculate the envelope function $\rho'(t)$ for the filtered record $\zeta'(t)$ from

$$\rho' = \pm(\zeta'^2 + \eta'^2)^{\frac{1}{2}}. \tag{7.10}$$

8. Examples

Figure 1*a* shows a typical section of a record of surface elevation taken in the southern North Sea by a ship-borne wave recorder. The record is digitized at time intervals of 1 s.

The spectrum of a stretch of the record lasting $19\frac{1}{2}$ min ($M = 1170$) is shown in figure 2. Each ordinate represents $\sum_n \frac{1}{2}c_n^2$ summed over 10 successive harmonics. The vertical scale has been normalized so that

$$\bar{\zeta} = a_M = 0 \tag{8.1}$$

and

$$\bar{\zeta^2} = \sum_{n=1}^{M} \tfrac{1}{2}c_n^2 = 1, \tag{8.2}$$

where $c_n^2 = a_n^2 + b_n^2$. It can be seen that, apart from the slight rise in energy at very low frequencies (which may be partly due to the method of measurement) there is a single dominant

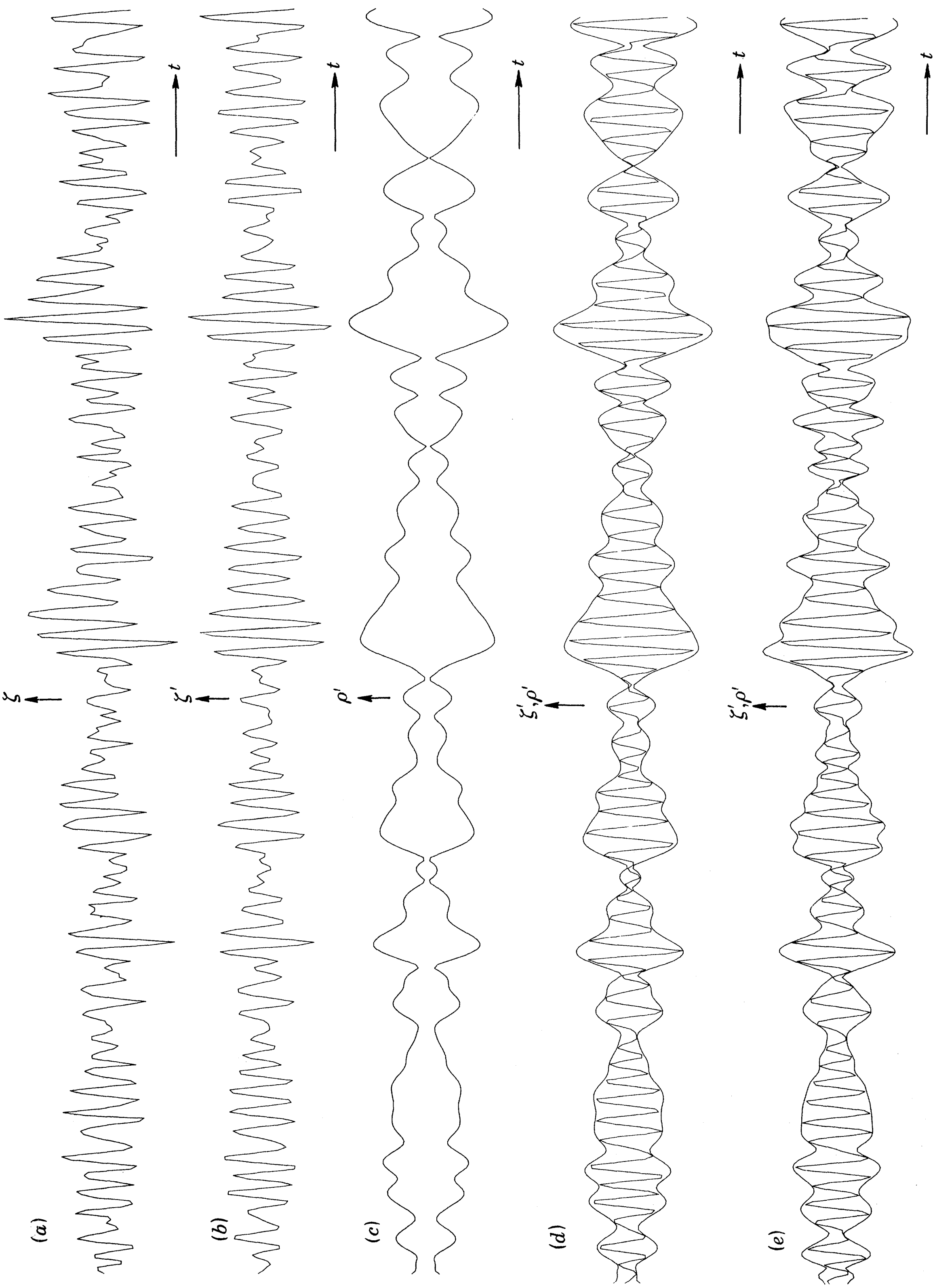

FIGURE 1. Part of a record of sea-surface elevation made with a shipborne wave recorder in the North Sea, at 55° 04 N, 7° 32 E, on 22 Sep. 1973. Digitization: 1 Hz. (*a*) original record; (*b*) filtered record: $n'/n_p = 0.5$, $n''/n_p = 1.5$; (*c*) envelope function (7.10) of (*b*). (*d*) superposition of (*b*) and (*c*). (*e*) As (*d*), but with $n'/n_p = 0.25$, $n''/n_p = 1.75$.

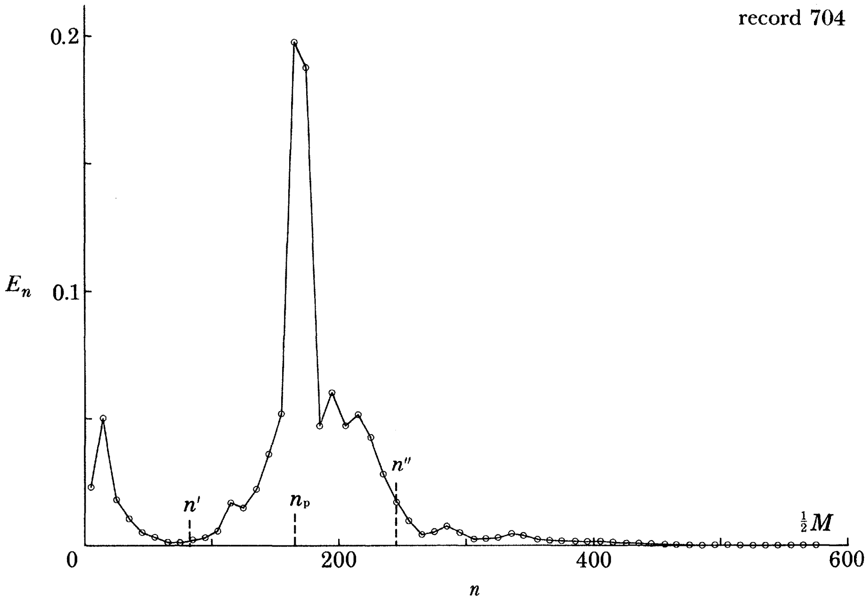

FIGURE 2. Frequency spectrum of the complete record shown partly in figure 1*a*.

peak in the spectrum at about $n = n_p = 165$ (corresponding to a frequency $n/M = 0.141$ Hz). On the high-frequency side, the energy falls away rapidly. For reasons mentioned in §1, the energy at $n > 2n_p$ is irrelevant to a study of dominant-wave grouping, if we neglect nonlinear effects.

Suppose we take the lower and upper cut-off frequencies at $n' = 0.5\,n_p$ and $n = 1.5\,n_p$, for example. Figure 1*b* shows the resulting filtered record ζ'. Corresponding crests and troughs of the dominant waves between figures 1*a* and *b* can easily be identified. The envelope function $\pm\rho'$ is shown by itself in figure 1*c*, and it will be noticed at once that there are a surprising number of points where ρ' seems to approach zero, so that the positive and negative branches cross over. The function $\zeta'(t)$ and its envelope are shown superimposed in figure 1*d*.

Figure 3*a* shows the total number of up-crossings of a given level ρ by the envelope function throughout the record (with the same choice of n', n''). The solid curve represents equation (3.9). The fit appears reasonable; statistical fluctuations might be expected to produce differences of order $(TN)^{\frac{1}{2}}$. It will be noticed that the maximum theoretical value $TN = 43$ is quite close to the value $TN = 45$ which is obtained if one constructs a visual envelope of the original record ζ by drawing straight lines between successive crests.

Figure 1*e* shows the effect of taking different cut-off frequencies, so that now $n = 0.25\,n_p$ and $n'' = 1.75\,n_p$. The envelope has many more fluctuations (maxima and minima) which seem to be irrelevant to the fluctuations in the height of the dominant waves. The corresponding number of level-crossings TN is shown in figure 3*b*. Again, the empirical points agree reasonably with the theoretical curve, but the maximum value of TN is now 56, or somewhat greater than the visual value.

Table 3 summarizes the results for various values of n'/n_p and n''/n_p. It will be seen that a change in n'/n_p from 0.5 to 0.25 has relatively little effect, but as n''/n_p is varied from 1.5 to 2.5, so TN departs more and more from the visual value.

Figure 4 shows the average number $\bar{G}$ of waves in a group, corresponding to figure 3*a*, that

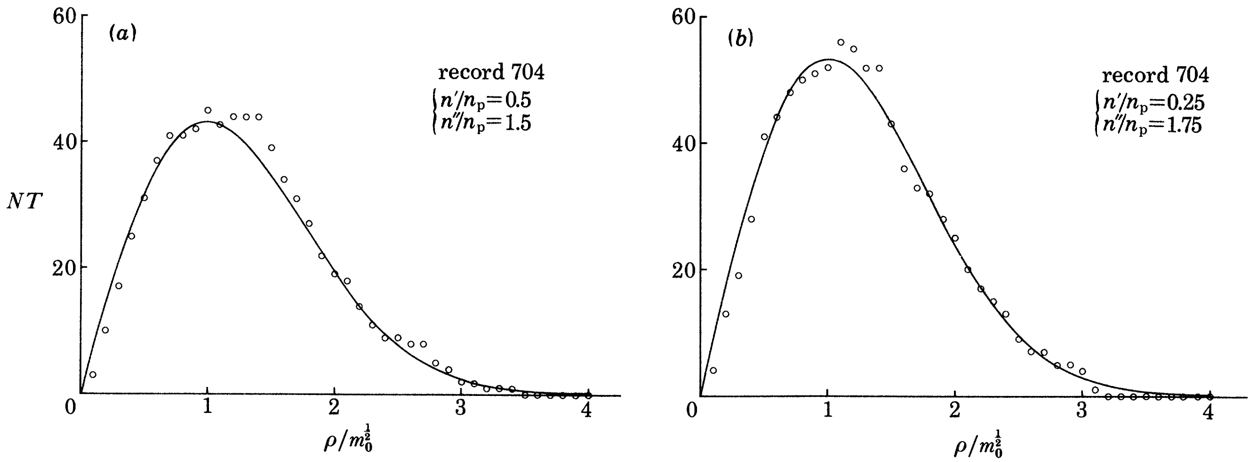

FIGURE 3. Number of level crossings of the wave envelope in the complete length of record shown partly in figure 1, as a function of the critical level (a) when $n'/n_p = 0.5$, $n''/n_p = 1.5$; (b) when $n'/n_p = 0.25$, $n''/n_p = 1.75$.

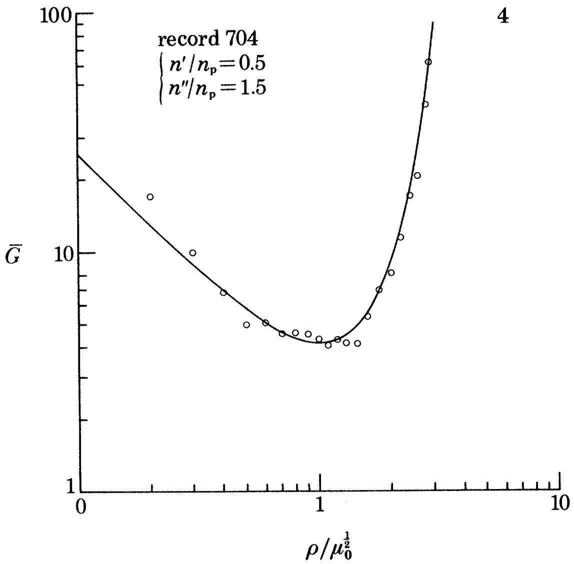

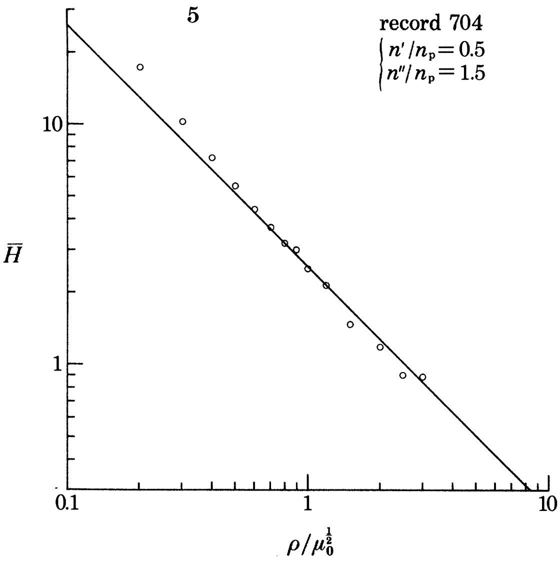

FIGURE 4. Plot of the mean group length $\bar{G}$ corresponding to figure 1*d*, as a function of the critical level. The theoretical curve represents (4.5).

FIGURE 5. Plot of the mean length of high runs $\bar{H}$ corresponding to the record of figure 1*d*. The line represents (5.5).

TABLE 3. SUMMARY OF THE EFFECT OF VARYING THE CUT-OFF FREQUENCIES n' AND n'' ON THE ANALYSIS OF THE RECORD IN FIGURE 1

				N'			
				$\rho_0 = m_0^{\frac{1}{2}}$		$\rho_0 = 2m_0^{\frac{1}{2}}$	
n'/n_p	n''/n_p	ν	$m_0^{\frac{1}{2}}$	theor.	obs.	theor.	obs.
0.50	1.50	0.160	15.5	43.2	45	19.3	19
0.50	1.75	.172	15.8	48.9	52	21.8	24
0.25	1.75	.196	15.9	53.4	56	23.8	25
0.25	2.00	.213	16.1	58.8	59	26.2	25
0.25	2.25	.237	16.2	66.1	69	29.5	26
0.25	2.50	.250	16.2	70.5	72	31.5	30
	visual				45		18.5

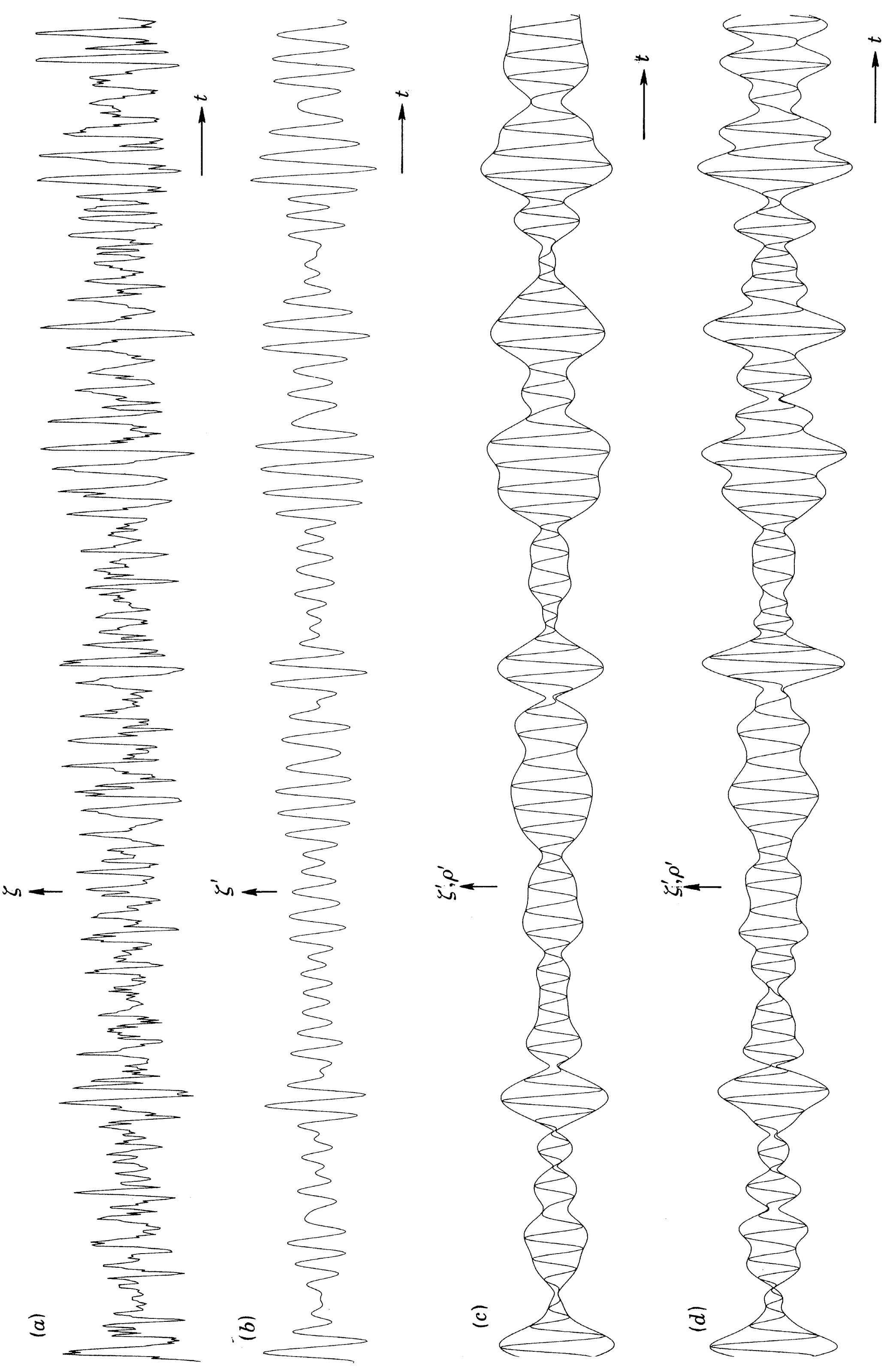

FIGURE 6. Part of a record of sea-surface elevation made with a surface wave follower at the Noordwijk Platform, 52° 16 N, 4° 8 E, on 18 Oct. 1979. Digitization: 1 Hz. (a) original record; (b) filtered record: $n'/n_p = 0.5$, $n''/n_p = 1.5$; (c) superposition of (b) and its envelope function; (d) as (c), but with $n'/n_p = 0.25$, $n''/n_p = 1.75$.

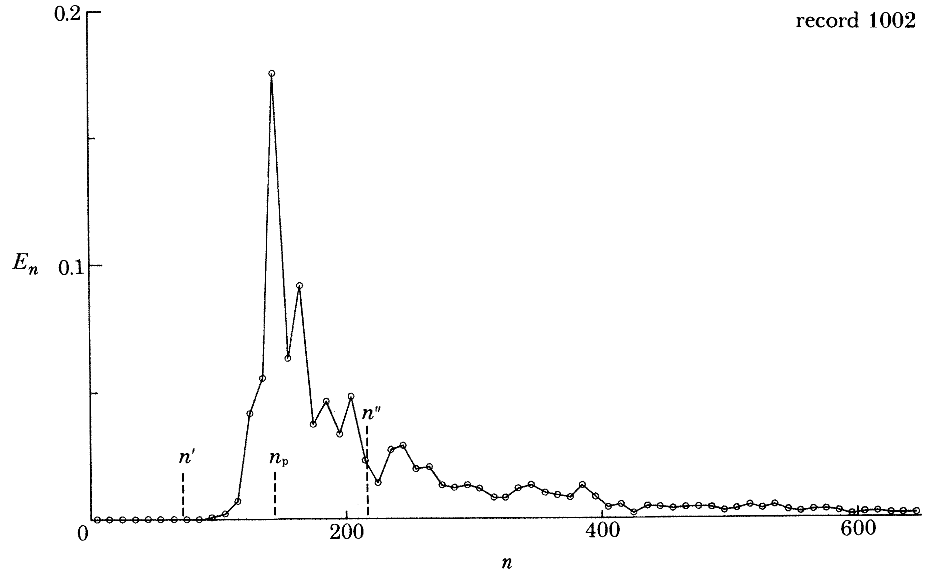

FIGURE 7. Frequency spectrum of the complete record shown partly in figure 6*a*.

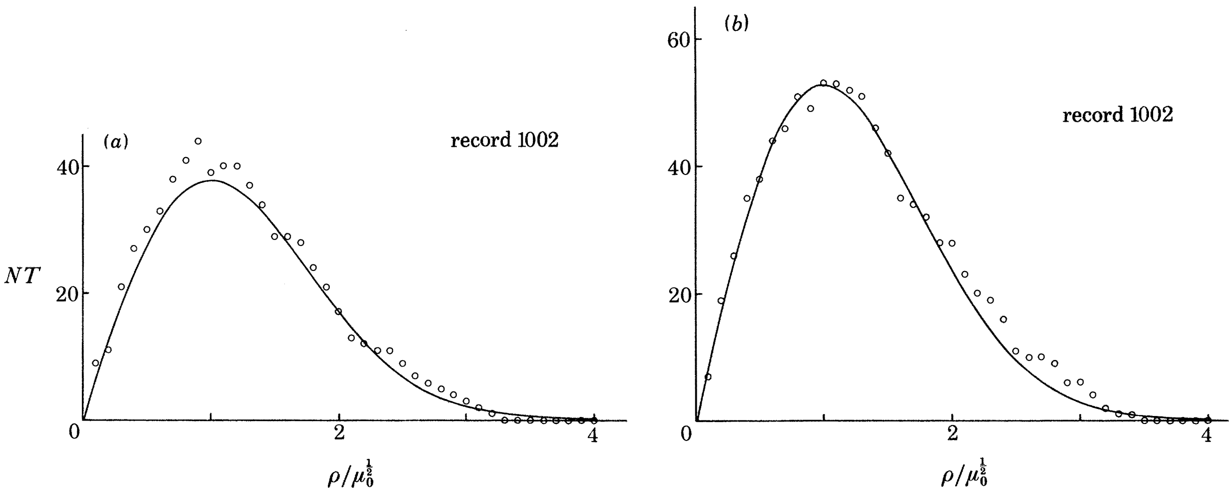

FIGURE 8. Number of level crossings of the wave envelope in the complete length of record shown partly in figure 6, as a function of the critical level (*a*) when $n'/n_p = 0.5$, $n''/n_p = 1.5$; (*b*) when $n'/n_p = 0.25$, $n''/n_p = 1.75$.

is to say when $n'/n_p = 0.5$ and $n''/n_p = 1.5$. The full curve represents the theory, equation (4.5). Except for very low levels ρ there is fair agreement. The minimum value $\bar{G}_{\min}$ at $\rho/\mu_0^{\frac{1}{2}} = 1$ is about 4.1, and at the significant wave amplitude ($\rho/\mu_0^{\frac{1}{2}} = 2$) $\bar{G}$ is about 9.2.

Figure 5 shows corresponding results for the mean number of waves $\bar{H}$ in a high run, given by equation (6.5). Though the two curves for $\bar{G}$ and $\bar{H}$ are quite different, the agreement between theory and observation is of course similar in figures 4 and 5.

As a second example, we show in figure 6*a* a typical wave record taken from the Nordwijk tower in the North Sea during MARSEN. The instrument used was the 'wave follower' described by Hsaio & Shemdin (1983). Figure 7 shows the spectral density function. This has a slightly longer high-frequency tail than the previous example, figure 2. However, if we take the cutoffs $n'/n_p = 0.5$ and $n''/n_p = 1.5$ we obtain the reasonably smooth envelope function shown in figure 6*c*. The wider cut-offs $n'/n_p = 0.25$, $n''/n_p = 1.75$ give the record in figure 6*d*, in which the envelope has a greater number of 'wiggles'. The corresponding numbers of level-crossings are shown in figures 8*a* and *b*. Again, there is fair agreement, but the scale value TN_{max} (at $\rho/\mu_0^{\frac{1}{2}} = 1$) agrees better with the visually determined value ($TN = 35$) when the cut-off limits are narrower ($n'/n_p = 0.5$, $n''/n_p = 1.5$). Graphs of $\bar{G}$ and $\bar{H}$ are shown in figures 9 and 10.

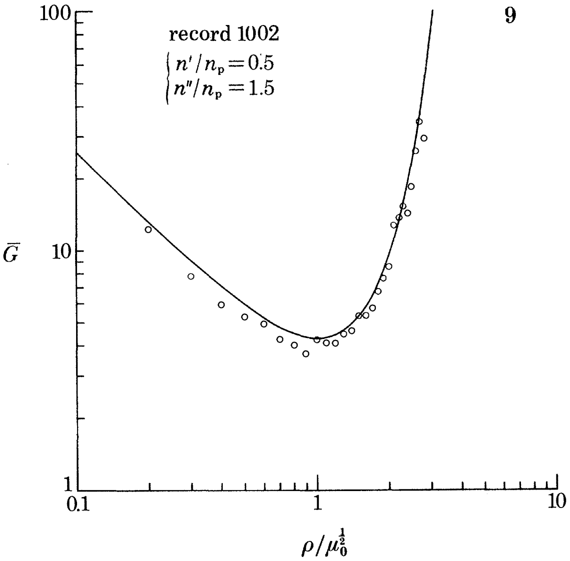

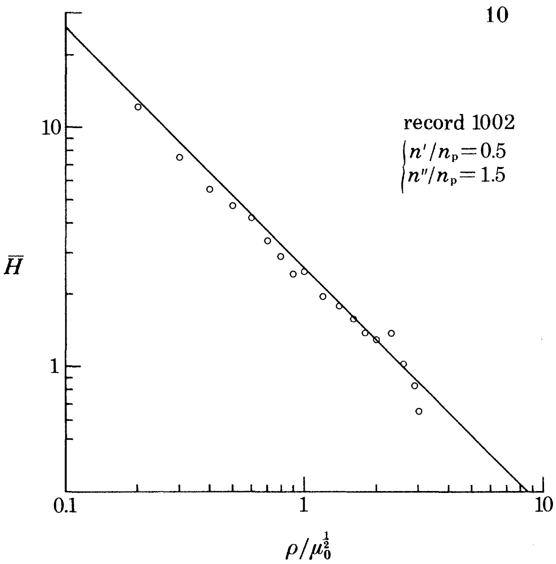

FIGURE 9. Plot of the mean group-length $\bar{G}$ corresponding to figure 6*c* as a function of the critical level. The theoretical curve represents (4.5).

FIGURE 10. Plot of the mean length of high runs $\bar{H}$ corresponding to figure 6*c*. The line represents (5.5).

From these examples we may conclude that typical wind-wave spectra are effectively filtered by a 'group analysis', and that the cut-off frequencies $n' = 0.5\, n_p$, $n'' = 1.5\, n_p$ are appropriate. As seen from table 3, this filtering of the record reduces slightly the total energy m_0 in the record. For a satisfactory analysis we may specify that m_0 shall not be changed significantly by the filtering. Such a limitation appears to be inherent in the idea of a wave-group analysis. For, any energy outside the dominant wave band is irrelevant to the quantities of interest. Thus, any spectrum that is not of the unimodal type, say one that has energy distributed in two or more widely separated frequency bands, is essentially unsuitable for simple group analysis. More complicated definitions may of course be sought.

9. The distribution of group lengths

The length l of a group was defined in §4 as the interval between two successive up-crossings of $\rho(t)$. The statistical distribution of l, apart from its mean $\bar{l}$, is difficult to determine in general (see Rice 1958). However, for narrow spectra an approximation may be derived from the notion that since the spectrum of ρ is predominantly low-pass, we expect successive up-crossings to be uncorrelated, at least when l is sufficiently large. Hence the distribution of l will be asymptotically the same as in a 'shot-effect', where the time-axis is peppered randomly with points at a mean rate

$$\lambda = 1/\bar{l} \tag{9.1}$$

per unit time. The density $p(l)$ for this process is known to be simply

$$p(l) = \lambda e^{-\lambda l}, \tag{9.2}$$

that is a negative exponential (see Rice 1954, section 3.4). Rice gives a proof involving an infinite series of terms. A more direct proof is as follows. Divide a given interval $(t, t+l)$ into a large number m of equal parts. The probability that ρ has no level crossing in any of these sub-intervals is $(1-\lambda l/m)^m$, and in the limit as $m \to \infty$ this tends to

$$P(l) = e^{-\lambda l}. \tag{9.3}$$

The density (9.2) then follows on applying the general formula

$$p(l) = (1/\lambda)\, d^2P/dl^2, \tag{9.4}$$

where λ is the mean number of up-crossings per unit time (see Longuet-Higgins 1958, section 2).

Incidentally it may be noted that for the low-pass spectrum $E(\sigma) = (1+\sigma^2)^{-2}$, the distribution of zero-crossing intervals of ζ is almost (but not quite) negative exponential; see Favreau *et al.* (1956); Longuet-Higgins (1962).

Assuming (9.2) to be valid, we have simply

$$p(l) = \bar{l}\, e^{-l/\bar{l}} \tag{9.5}$$

and so for the number of waves G in a complete group

$$p(G) = \bar{G}\, e^{-G/\bar{G}}, \tag{9.6}$$

where $\bar{G}$ is given by (4.8). Some comparisons with observation will be given below.

The question arises as to what meaning we should attach to a fractional number of waves in a group. This can occur because the wave envelope ρ may exceed the reference level for only a short interval of time. In any given case a wave crest may or may not be present during the interval. However, the fractional number of waves is still a measure of the *probability* of a wave crest exceeding the given level in that interval. As a matter of fact, owing to the dispersive properties of gravity waves, the phase velocity is greater than the group velocity. Hence any particular wave tends to advance through the group, and any section of the envelope contains a wave crest at least some of the time.

To estimate the statistical density $p(H)$ of high runs, we may assume as an approximation that each high run H is, on the whole, in proportion to the corresponding group length G, so $H = qG$, where q is given by (5.1). It follows that the distribution of H, like that of G, is also a negative exponential:

$$p(H) \doteqdot \bar{H}\, e^{-H/\bar{H}}. \tag{9.7}$$

Does this fit existing observations? Most data are given for integer values of the group length G or run length H. We may reasonably assume that the probability H_j of H for an integer value $j > 0$ is related to the continuous probability density $p(H)$ by

$$H_j \propto \int_{j-\frac{1}{2}}^{j+\frac{1}{2}} p(H)\, dH, \tag{9.8}$$

that is to say, the probability density of a run of length H contributes to the probability of the discrete run having the nearest integar value. The densities for runs H less than $\frac{1}{2}$ contribute only to runs of zero length, that is they are ignored.

If $p(H)$ is a negative exponential, then the assumption (9.8) has two simple consequences: (1) the probability H_j is also negative exponential, that is

$$H_j \propto e^{-j/\overline{H}}, \tag{9.9}$$

and (2) because of the effective truncation of the distribution at $H = \frac{1}{2}$, the mean value $\overline{H}_j$ is increased by approximately the same amount, i.e.

$$\overline{H}_j \doteqdot \overline{H} + 0.5. \tag{9.10}$$

Sufficiently long wave records are quite rare, but the numerically simulated data of Kimura (1980), reproduced in part in figures 17 and 18 below, show conclusively that the distribution of H_j is indeed negative exponential, over practically the whole range of j. Figures 19 and 20 show that the distribution of G_j is almost exponential, particularly when j is large, as expected, but for small values of j there are systematic differences.

For H_j it is therefore worth testing the second conclusion (9.8) just mentioned. The 'target spectra' used by Kimura (1980) and shown in his figure 8 appear to be of the form

$$S(f) = f^{-n}\, e^{(n/\gamma)(1-f^{-\gamma})} \qquad (f = \sigma/2\pi), \tag{9.11}$$

where $\gamma = 4$ and n runs from 4 to 8 in Kimura's cases 1 to 5, respectively. It will be seen that the analytic form (9.11) has a peak at $f = f_p = 1$, where $S = S_{max} = 1$, as required.

TABLE 4. COMPARISON OF THEORETICAL AND OBSERVED VALUES OF THE MEAN PROBABILITY $\overline{H}_l$ OF HIGH RUNS, IN THE DATA OF KIMURA (1980)

			$\rho = \rho_{mean}$			$\rho = \rho_{\frac{1}{3}}$		
case	n	ν'	$\overline{H}$	$\overline{H}_j$	data	$\overline{H}$	$\overline{H}_j$	data
1	4	0.1879	1.72	2.22	2.20	1.08	1.58	1.28
2	5	.1805	1.82	2.32	2.29	1.12	1.62	1.29
3	6	.1742	1.85	2.35	2.34	1.16	1.66	1.29
4	7	.1686	1.92	2.42	2.42	1.20	1.70	1.37
5	8	.1635	1.96	2.46	2.45	1.23	1.73	1.53

With cut-off frequencies at $f = 0.5$ and 1.5, we calculate the values of ν, $\overline{H}$ and $\overline{H}_j$ seen in table 4, both for $\rho = \rho_{mean}$ $(\rho/\mu_0^{\frac{1}{2}} = \surd(2/\pi))$ and for $\rho = \rho_{\frac{1}{3}}$ $(\rho/\mu_0^{\frac{1}{2}} = 2)$. Comparison with the data, taken from table 1 of Kimura (1980) shows good agreement when $\rho = \rho_{mean}$, though less so when $\rho = \rho_{\frac{1}{3}}$.

In the following three sections (§§10–12) we shall outline a different approach for finding the distributions of H_j and G_j, based partly on the work of Kimura (1980), but with some significant modifications.

10. Correlation between successive wave heights

Consider the joint density of $\rho_1 = \rho(t_1)$ and $\rho_2 = \rho(t_2)$ at two points separated by a constant time interval $\tau = t_2 - t_1$. This is known exactly from the work of Uhlenbeck (1943) and Rice (1944, 1958). The general result may be written

$$p(\rho_1, \rho_2) = \frac{\rho_1 \rho_2}{\mu_0^2(1-\kappa^2)} \mathrm{e}^{-(\rho_1^2+\rho_2^2)/2\mu_0(1-\kappa^2)} I_0\left(\frac{\kappa}{1-\kappa^2}\frac{\rho_1\rho_2}{\mu_0}\right), \tag{10.1}$$

where

$$\left.\begin{aligned} X &= \int_0^\infty E(\sigma)\cos(\sigma-\bar{\sigma})\,\tau\,\mathrm{d}\sigma, \\ Y &= \int_0^\infty E(\sigma)\sin(\sigma-\bar{\sigma})\,\tau\,\mathrm{d}\sigma, \end{aligned}\right\} \tag{10.2}$$

$$\kappa = (X^2+Y^2)^{\frac{1}{2}}/\mu_0, \tag{10.3}$$

and I_0 denotes the modified Bessel function of order zero:

$$I_0(z) = \frac{1}{2\pi}\int_0^{2\pi} \mathrm{e}^z \cos\theta\,\mathrm{d}\theta. \tag{10.4}$$

When $\kappa = 0$ then $p(\rho_1, \rho_2)$ reduces to the product of two Rayleigh distributions: $p(\rho_1)\,p(\rho_2)$.

We shall assume that when the separation τ equals $2\pi/\bar{\sigma}$, then ρ_1 and ρ_2 approximate the amplitudes of two successive waves.

The correlation coefficient γ, defined as $M_{11}/(M_{20}M_{02})^{\frac{1}{2}}$ where

$$M_{pq} = \int_0^\infty\int_0^\infty (\rho_1-\bar{\rho})^p(\rho_2-\bar{\rho})^q p(\rho_1,\rho_2)\,\mathrm{d}\rho_1\,\mathrm{d}\rho_2, \tag{10.5}$$

has been evaluated by Uhlenbeck (1943); see also Middleton (1960), as

$$\gamma = [E - \tfrac{1}{2}(1-\kappa^2)\,K - \tfrac{1}{4}\pi]/(1-\tfrac{1}{4}\pi), \tag{10.6}$$

where E and K are complete elliptic integrals:

$$E(\kappa) = \int_0^{\frac{1}{2}\pi}(1-\kappa^2\sin^2\theta)^{\frac{1}{2}}\,\mathrm{d}\theta, \tag{10.7}$$

and

$$K(\kappa) = \int_0^{\frac{1}{2}\pi}(1-\kappa^2\sin^2\theta)^{-\frac{1}{2}}\,\mathrm{d}\theta. \tag{10.8}$$

γ is shown as a function of κ^2 in figure 11 (cf. Kimura 1980, figure 1, where γ is shown as a function of κ).

For values of κ very close to 1 it may be shown that

$$\gamma \sim 1-(1-\kappa^2)/(4-\pi), \tag{10.9}$$

and this is represented by the tangent at $\kappa = 1$ to the curve in figure 11. However, it can be seen immediately that for values of κ^2 less than 0.6 a closer approximation to γ is given by the simple expression

$$\gamma \doteqdot \kappa^2 \tag{10.10}$$

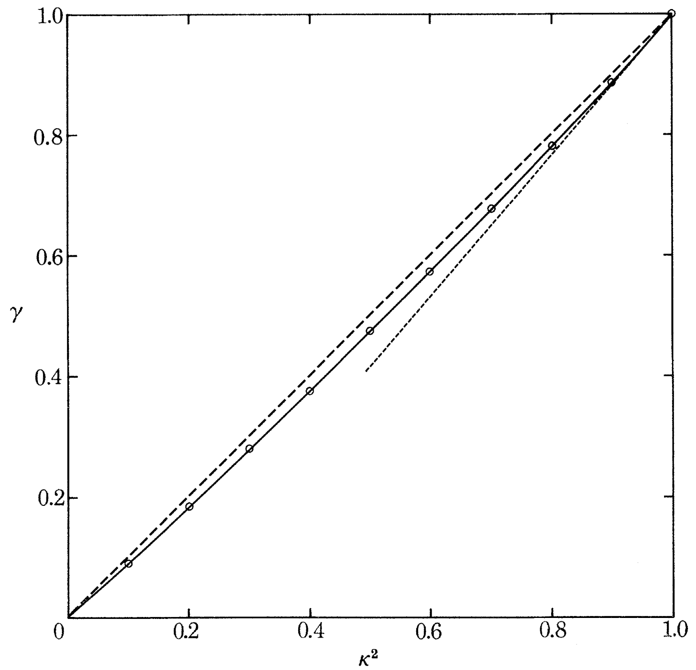

FIGURE 11. The correlation coefficient γ between ρ_1 and ρ_2 shown as a function of the parameter κ^2.

represented by the straight diagonal in figure 11. This holds good to within a small percentage over the whole range of κ.

Consider the interpretation of these results for a narrow spectrum. From (2.10) and (2.7) we have

$$\mu_0^2 = \int_0^\infty \int_0^\infty E(\sigma)\, E(\sigma')\, \mathrm{d}\sigma\, \mathrm{d}\sigma' \tag{10.11}$$

and similarly from (10.2)

$$X^2 + Y^2 = \int_0^\infty \int_0^\infty E(\sigma)\, E(\sigma') \cos(\sigma - \sigma')\, \tau\, \mathrm{d}\sigma\, \mathrm{d}\sigma'. \tag{10.12}$$

So by (10.3)

$$\mu_0^2(1-\kappa^2) = 2\int_0^\infty \int_0^\infty E(\sigma)\, E(\sigma') \sin^2 \tfrac{1}{2}(\sigma - \sigma')\, \tau\, \mathrm{d}\sigma\, \mathrm{d}\sigma'. \tag{10.13}$$

For a narrow spectrum let us formally replace the trigonometric term in (10.12) by the first term in its power series, that is set

$$\sin^2 \tfrac{1}{2}(\sigma - \sigma')\, \tau \doteqdot \tfrac{1}{4}(\sigma - \sigma')^2 \tau^2 \tag{10.14}$$

$$= \tfrac{1}{4}[(\sigma - \bar{\sigma})^2 - (\sigma' - \bar{\sigma})^2]\, \tau^2. \tag{10.15}$$

Then we obtain

$$\mu_0^2(1-\kappa^2) \doteqdot \tfrac{1}{2}(\mu_2\mu_0 - 2\mu_1^2 + \mu_0\mu_2) = \mu_0\mu_2\, \tau^2, \tag{10.16}$$

since $\mu_1 = 0$. Hence writing

$$\tau = 2\pi/\bar{\sigma} \tag{10.17}$$

we see from (10.13) that, to lowest order,

$$1 - \kappa^2 = (\mu_2/\mu_0)\, \tau^2 = 4\pi^2\nu^2. \tag{10.18}$$

So from (10.9)

$$\gamma \doteqdot 1-45.99\,\nu^2, \tag{10.19}$$

Because of the coefficient $4\pi^2$ in (10.19) this formula for γ can be expected to be adequate only when $\nu < 0.1$, say. A similar limitation on the value of ν arises from the representation of the sinusoidal term in (10.13) by a single term $\frac{1}{4}(\sigma-\sigma')^2\tau^2$. This can be valid at best only so long as $|\sigma-\sigma'|\tau < \frac{1}{2}\pi$. But for substitution in the double integral (10.15), we should require $|\sigma-\sigma'|$ to be at least as great as twice the spectral width $(\mu_2/\mu_0)^{\frac{1}{2}}$. Hence

$$2(\mu_2/\mu_0)^{\frac{1}{2}}\tau < \tfrac{1}{2}\pi, \tag{10.20}$$

which with τ given by (10.19) is equivalent to

$$(\mu_2/\mu_0)^{\frac{1}{2}} < \tfrac{1}{8}\bar{\sigma}, \tag{10.21}$$

that is

$$\nu < 0.125. \tag{10.22}$$

If we wished to calculate the correlation γ_2 between *alternate* wave heights, we would have to substitute $\tau = 4\pi/\bar{\sigma}$ in (10.16), thus doubling τ and restricting the range of validity of the linear theory to $\nu < 0.025$, at most. None the less the linearized theory does suggest qualitatively the very drastic reduction in γ to be expected as ν and τ are increased beyond the limits estimated above.

For larger values of ν or τ we may use the accurate expressions for κ^2 provided by (10.2) and (10.3), together with the relation between γ and κ indicated by the solid curve in figure 11, or its approximation, equation (10.10). Alternatively, κ may be determined directly from observation since it is equal to coefficient of correlation between ρ_1^2 and ρ_2^2.

11. The correlation coefficient: examples

To illustrate the dependence of κ on ν for typical spectra, consider the band-pass spectrum (6.1), for which $\nu = 3^{-\frac{1}{2}}\delta$. From (10.1) we have immediately

$$X = m_0(\sin\delta\bar{\sigma}\tau)/\delta\bar{\sigma}\tau, \quad Y = 0. \tag{11.1}$$

Hence

$$\kappa^2 = [(\sin\delta\bar{\sigma}\tau)/\delta\bar{\sigma}\tau]^2. \tag{11.2}$$

To find $\gamma = \gamma_1$, write $\tau = 2\pi/\bar{\sigma}$, so

$$\kappa^2 = [(\sin 2\pi\delta)/2\pi\delta]^2. \tag{11.3}$$

As $\delta \to 0$ we have $\kappa^2 = 1-\frac{4}{3}\pi^2\delta^2$, in agreement with (10.20). As δ increases from 0, at first κ^2 decreases monotonically to 0 at $\delta = 0.5$ ($\nu = 0.289$). However, as δ increases further, κ^2 rises again to a maximum value 0.047 before falling finally to zero at $\delta = 1$ ($\nu = 0.577$).

In figure 12 we also show κ_m, the correlation coefficient corresponding to $\tau = 2m\pi/\bar{\sigma}$. This shows that $\gamma_2 < \gamma_1$ always, but as m increases, it is not always true that $\gamma_{m+1} < \gamma_m$. For instance when $\nu = 1.4$, γ_3 may exceed γ_2.

This non-monotonic behaviour may be associated with the sharp cut off in a band-pass spectrum. An example when the cut-off is smooth, but still decisive, is provided by the 'ocean-swell' spectrum (6.3). For this spectrum it may be shown that

$$\kappa^2 = (1+r^2)^{-\frac{1}{2}}\,e^{-2n\{[\frac{1}{2}(1+r^2)^{\frac{1}{2}}+\frac{1}{2}]^{\frac{1}{2}}-1\}} \tag{11.4}$$

where

$$r = 4m\pi/(n+1). \tag{11.5}$$

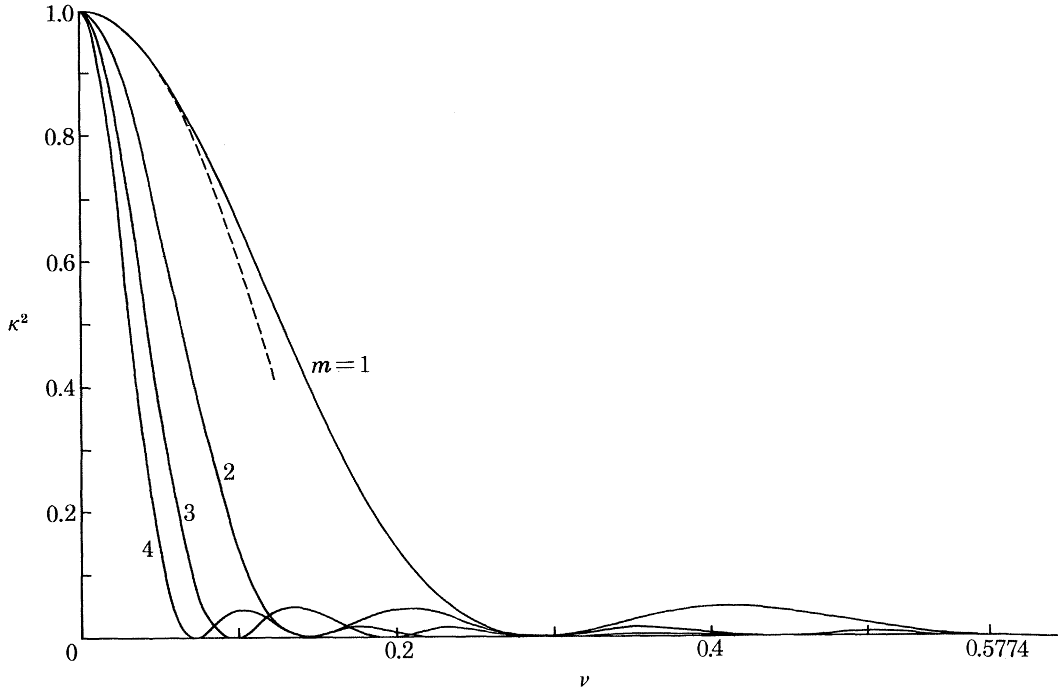

FIGURE 12. κ^2 as a function of ν for the band-pass spectrum (6.1). The broken curve represents the asymptote (10.18) when $m = 1$.

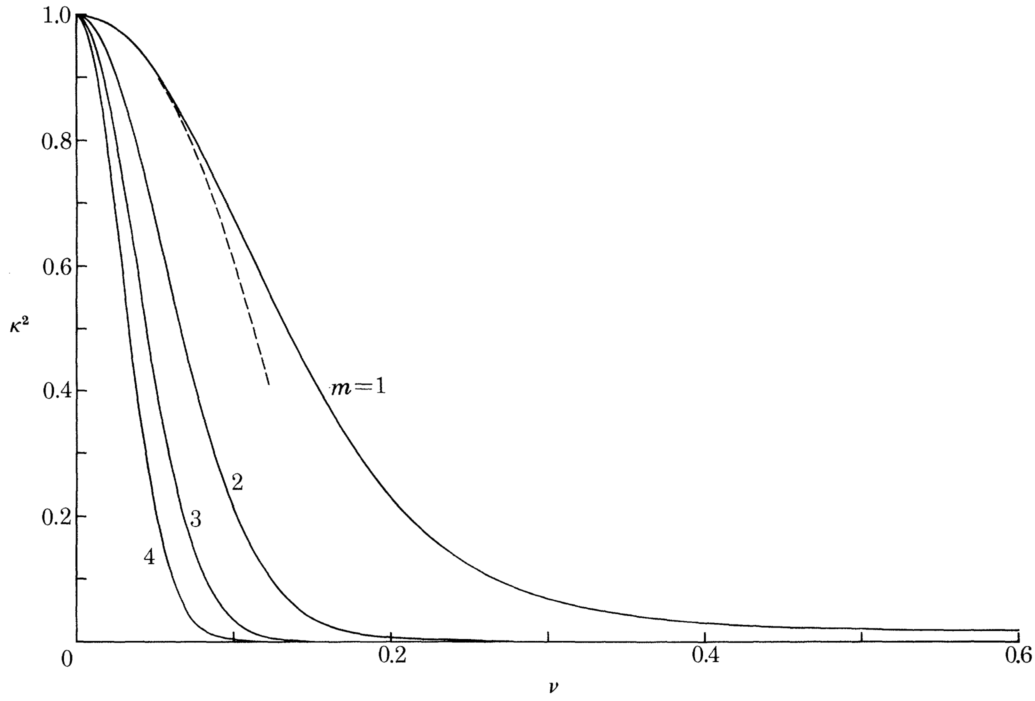

FIGURE 13. κ^2 as a function of ν for the 'ocean swell spectrum' (6.3). The broken curve represents the asymptote (10.18) when $m = 1$.

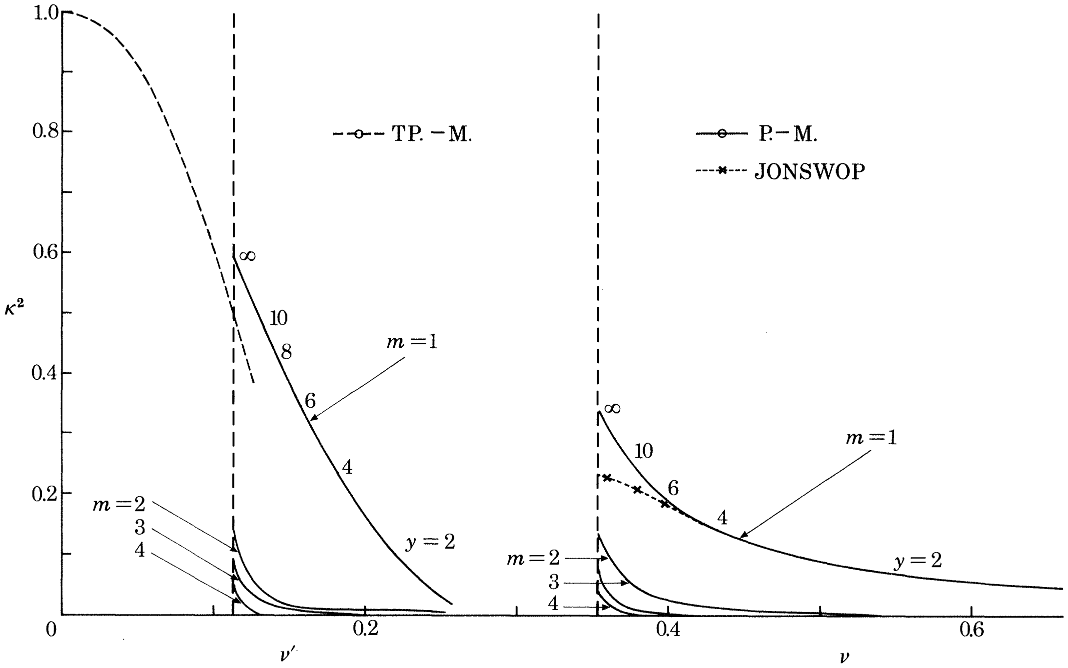

FIGURE 14. κ^2 as a function of ν for the Pierson–Moskowitz spectrum (P.–M.), and JONSWAP spectrum. These are on the right. The corresponding curves for the truncated Pierson–Moskowitz spectrum (TP.–M.) are shown on the left.

The expression (11.4) is plotted against ν in figure 13. Each curve is now monotonic in both ν and m, over the ranges shown, and when $\nu > 0.15$, γ_2, γ_3 and γ_4 are all very small.

When $\nu = 0.082$, for example, the sequence of values of κ^2 for $m = 1, 2, 3$ and 4 is 0.76, 0.34, 0.10 and 0.02, giving $\gamma_m = 0.74, 0.32, 0.10$ and 0.02. This compares with Goda's (1983) values for swell of $\gamma_m = 0.65, 0.35, 0.18$ and 0.07.

For wind-waves, however, very different results are to be expected. Figure 14 shows κ^2 plotted against ν for the Pierson–Moskowitz spectrum, equation (6.9). In general, the integrals X and Y of (10.2) were found by quadratures, through in two cases the numerical values could be checked against explicit expressions. For in the case $\gamma = \infty$ (the Phillips spectrum), integration of (10.2) by parts gives

$$X+\mathrm{i}Y = \frac{1}{24}\left[(6+2\mathrm{i}\tau-\tau^2-\mathrm{i}\tau^3)\,\mathrm{e}^{\mathrm{i}\tau}+\tau^4\int_\tau^\infty \frac{\mathrm{e}^{\mathrm{i}u}}{u}\,\mathrm{d}u\right], \tag{11.6}$$

the last function being tabulated in Abramowitz & Stegun (1965), table 5.3. Also when $\gamma = 1$, we find from Erdelyi (1954) (1.4.21) and (2.4.31) that

$$X+\mathrm{i}Y = 2\alpha(\tau/\beta)^2\,K_4(z), \tag{11.7}$$

where $z = 2(\mathrm{i}\beta\tau)^{\frac{1}{2}}$ and K_4 denotes the modified Bessel function of order four (see Erdelyi 1953, ch. 8).

The behaviour of κ^2 shown in figure 14 differs from that in figure 13. For one thing, the value of ν for the Pierson–Moskowitz spectrum is never less than 0.3536. Also the maximum value of κ^2 is always less than 0.34. It is clear that for this spectrum the narrow-band expression (10.18) never applies.

However, for the truncated Pierson–Moskowitz spectrum, as shown on the left of figure 14, the situation is again different. The lower bound for ν' is now reduced to 0.113 (see table 2) and κ^2 can be as great as 0.595 compared with the narrow-band approximation 0.500. The sequence of values for γ_1, γ_2, γ_3, γ_4 is then 0.595, 0.139, 0.080 and 0.052. However, only a slight shift to the right, to say $\nu' = 0.16$ reduces γ_1 to about 0.33, which is typical of wind-waves. Further, γ_2, γ_3 and γ_4 are each reduced to less than 0.01, which can be considered insignificant.

12. Distribution of G_j and H_j: Markov theory

Kimura (1980) has given a rough but simple theory for the distribution of group lengths and of high runs, treating the sequence of wave-heights as a Markov chain, as first suggested by Sawnhey (1962). Kimura's theory can be presented in an even simpler way, without the use of matrices, as follows.

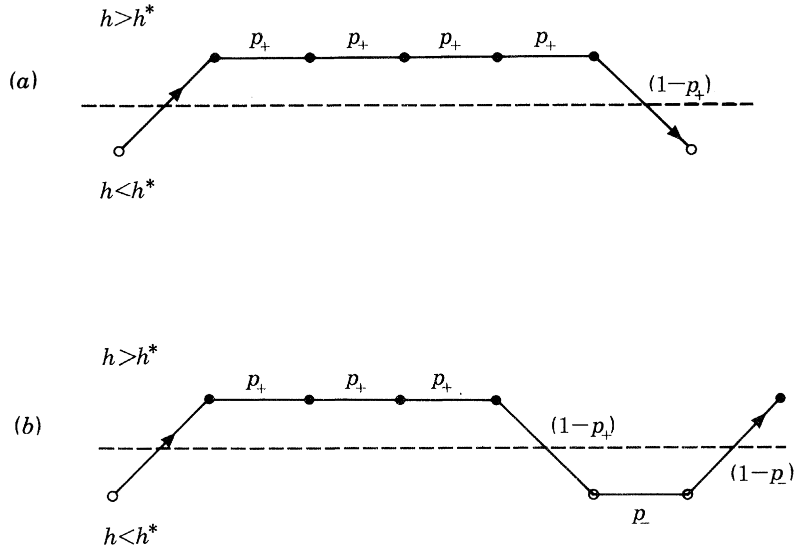

Figure 15. Diagram showing the basis for (a) the probability of a high run of j waves (12.1) when $j = 5$, and (b) the probability of a wave group of j waves, (12.3) and (12.4) when $i = 4, j = 6$.

Choose a critical wave-height h^* as in figure 15. Given that a certain wave-height h_1 exceeds h^*, let p_+ denote the probability that the next wave-height h_2 also exceeds h^*. To determine the probability of a high run of length j we know already that the first wave-height exceeds h^*; the next $(j-1)$ wave-heights must then exceed h^* and the one after must *not* exceed h^* (see figure 15a). The probabilities being assumed independent, the combined probability is

$$p(H_j) = p_+^{j-1}(1-p_+). \tag{12.1}$$

The mean length of high runs is then given by

$$\bar{H} = \sum_1^{\infty} jp(H_j) = 1/(1-p_+). \tag{12.2}$$

To find the distribution of total runs we may reason as follows. In a total run of length j the first i waves, say, will be a high run of length i and the remaining $(j-i)$ waves will be a low run of length $(j-i)$ (see figure 15b). The probability of such an event is clearly

$$p_+^{i-1}(1-p_+)\,p_-^{j-i-1}(1-p_-),\tag{12.3}$$

where p_- denotes the probability that $h_2 < h^*$ given that $h_1 < h^*$. Summing the above expression from $i = 1$ to $i = j-1$ we obtain

$$p(G_j) = (1-p_+)\,(1-p_-)\,(p_+^{j-1}-p_-^{j-1})/(p_+-p_-)\tag{12.4}$$

when $n \geqslant 2$. The mean length of a total run is then

$$\bar{G} = \sum_2^\infty jp(G_j) = 1/(1-p_+)+1/(1-p_-).\tag{12.5}$$

The only question then is to determine p_+ and p_- for a given wave record.

Kimura (1980) proposed that $p(h_1, h_2)$ be approximated by a two-dimensional Rayleigh distribution of the form (10.1), which is reasonable if we assume that h_1 and h_2 can be approximated by $2\rho_1$ and $2\rho_2$ respectively (though Kimura does not make this assumption explicitly). Then the conditional probabilities p_+ and p_- can be calculated directly from

$$\left.\begin{aligned} p_+ &= \int_{\rho^*}^\infty \int_{\rho^*}^\infty p(\rho_1,\rho_2)\,\mathrm{d}\rho_1\,\mathrm{d}\rho_2 \Big/ \int_0^\infty \int_{\rho^*}^\infty p(\rho_1,\rho_2)\,\mathrm{d}\rho_1\,\mathrm{d}\rho_2, \\ p_- &= \int_0^{\rho^*} \int_0^{\rho^*} p(\rho_1,\rho_2)\,\mathrm{d}\rho_1\,\mathrm{d}\rho_2 \Big/ \int_0^\infty \int_0^{\rho^*} p(\rho_1,\rho_2)\,\mathrm{d}\rho_1\,\mathrm{d}\rho_2, \end{aligned}\right\}\tag{12.6}$$

where $\rho^* = \frac{1}{2}h^*$. Such probabilities are then a function only of κ^2, as shown in figure 16. Here we plot p_+ and p_- against κ^2, and not against γ as was done by Kimura (1980).

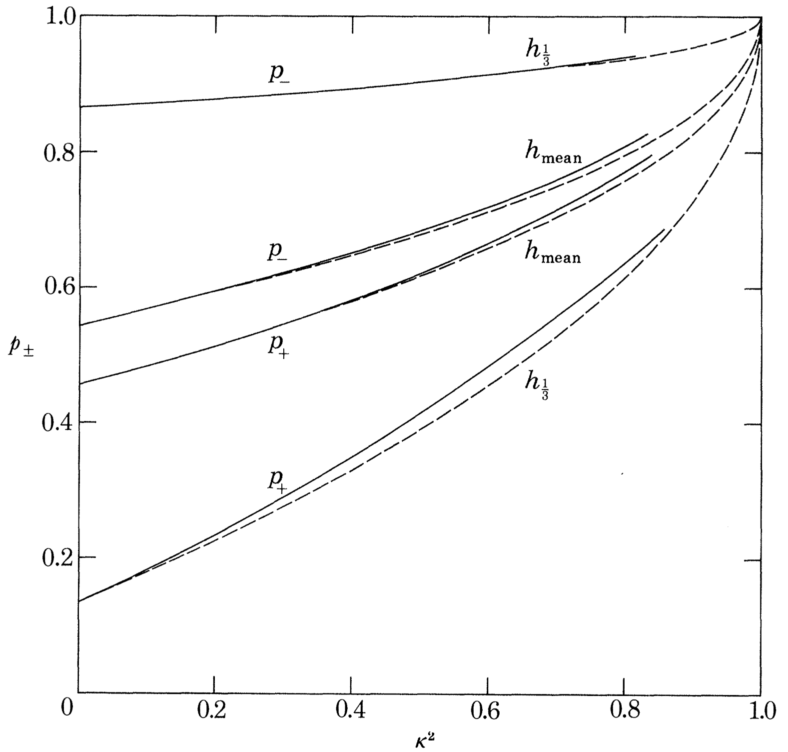

FIGURE 16. Graphs of p_+ and p_- as functions of κ^2 according to (12.6) and §10. The dashed curves represent the parabolic approximations (12.8).

Table 5*a*. Parameters of the Kimura spectrum (9.12)

					h_{mean}		$h_{\frac{1}{3}}$	
case	n	ν	κ^2	γ	p_+	p_-	p_+	p_1
1	4	0.8319	0.1253	0.116	0.490	0.574	0.194	0.874
2	5	.6980	.1513	.140	.498	.581	.207	.876
3	6	.6118	.1820	.169	.507	.589	.225	.879
4	7	.5507	.2152	.200	.517	.598	.242	.881
5	8	.5047	.2493	.232	.528	.606	.260	.883

Table 5*b*. Parameters of the truncated Kimura spectrum

					h_{mean}		$h_{\frac{1}{3}}$	
case	n	ν	κ^2	γ	p_+	p_-	p_+	p_-
1	4	0.5857	0.2071	0.192	0.516	0.595	0.237	0.880
2	5	.5453	.2412	.224	.526	.604	.256	.883
3	6	.5113	.2723	.254	.535	.613	.275	.885
4	7	.4820	.3011	.281	.545	.620	.292	.888
5	8	.4565	.3284	.307	.555	.628	.308	.890

Table 5*c*. Mean values of H_j for the truncated Kimura spectrum

	h_{mean}		$h_{\frac{1}{3}}$	
case	(12.2)	obs.	(12.5)	obs.
1	1.96	2.20	1.16	1.28
2	1.99	2.29	1.26	1.29
3	2.03	2.34	1.29	1.29
4	2.07	2.42	1.32	1.37
5	2.12	2.45	1.35	1.53

Table 5*d*. Mean values of G_j for the truncated Kimura spectrum

	h_{mean}		$h_{\frac{1}{3}}$	
case	(12.2)	obs.	(12.2)	obs.
1	4.31	4.66	9.18	9.33
2	4.38	4.67	9.33	9.47
3	4.46	4.94	9.55	10.00
4	4.56	5.17	9.72	9.95
5	4.66	5.32	9.90	10.71

Assuming that Kimura's five 'target spectra' are given by (9.12), we have calculated (see table 5*a*) the corresponding values of κ^2 and hence of p_+ and p_- from figure 16. The corresponding values for the truncated spectra are given in table 5*b*. It will be seen that while the truncation changes the values of ν, κ^2 and γ very considerably, the values of p_+ and p_- are much less affected†.

The distributions of G_j and H_j corresponding to the two extreme spectra (cases 1 and 5) are seen in figures 17–20. Also shown are Kimura's observations. From these results we may conclude

(1) that truncation of the spectra has a small but appreciable effect upon the theoretical distributions,

† The values of γ used by Kimura (1980) to calculate p_+ and p_- were determined empirically, and not calculated from the frequency spectra as here.

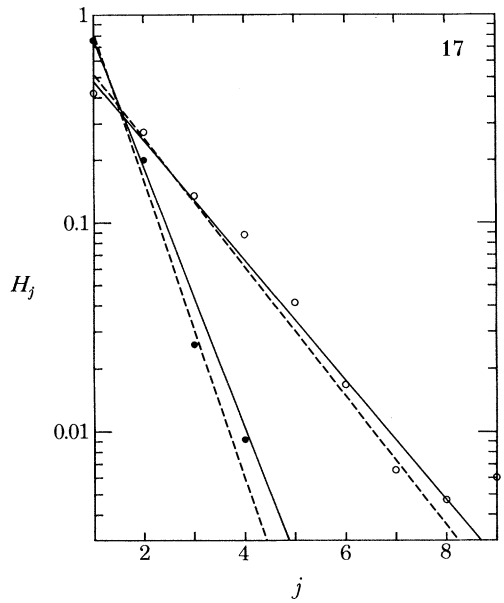

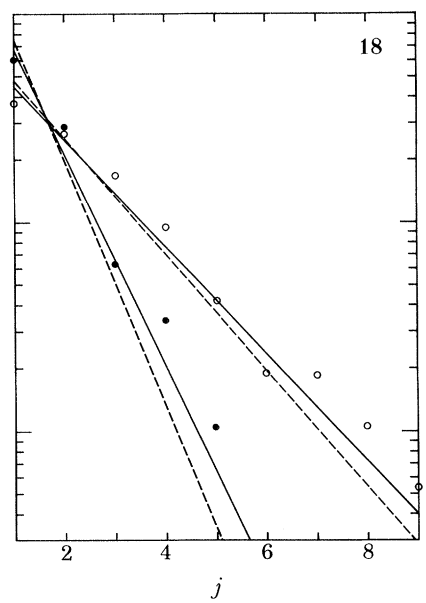

FIGURE 17. The probability H_j of a high run, as a function of j for the Kimura spectrum (9.12) when $n = 4$. The curves represent (12.1): ---, original spectrum; ——, truncated spectrum. Plotted points are data from Kimura (1980), figure 9*a*.

FIGURE 18. As figure 17, but with $n = 8$. The plotted points are from Kimura (1980), figure 9*e*.

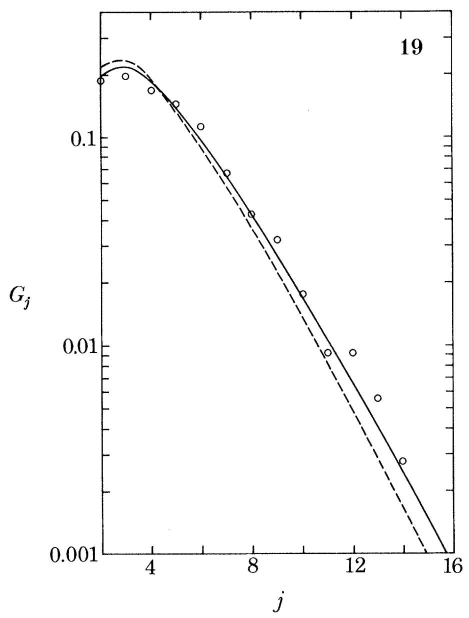

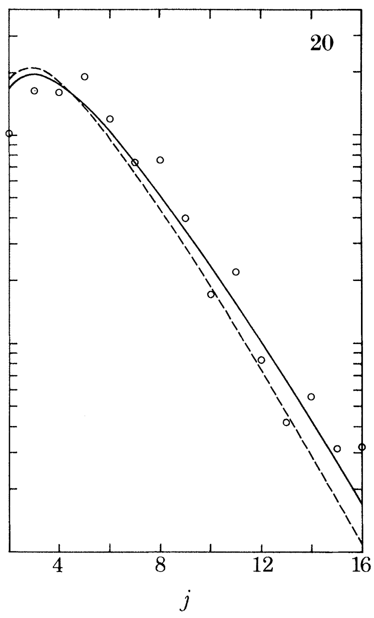

FIGURE 19. The probability G_j of a group of total length j for the Kimura spectrum (9.12) when $n = 4$. The curves represent (12.4): ---, original spectrum; ——, truncated spectrum. Plotted points are data from Kimura (1980), figure 10*a*.

FIGURE 20. As in figure 19, but with $n = 8$. The plotted points are from Kimura (1980), figure 10*e*.

(2) that the observations agree fairly well with either set of curves, but distinctly better with those for the truncated spectra (solid lines).

Based on figure 16, we may also give some rough analytic expressions for $\overline{H}$ and $\overline{G}$. For the values of p_+ and p_- on the left axis ($\gamma = 0$) are known:

$$p_+ = e^{-\frac{1}{2}\xi^2}, \quad p_- = 1 - e^{-\frac{1}{2}\xi^2}, \tag{12.7}$$

where $\xi = \rho/\mu_0^{\frac{1}{2}}$. If we approximate the curves in figure 16 by parabolas through the point $(1, 1)$ with horizontal axes we must have in general

$$\left.\begin{aligned} 1-p_+ &= (1-e^{-\frac{1}{2}\xi^2})\,(1-\kappa^2)^{\frac{1}{2}} \\ 1-p_- &= e^{-\frac{1}{2}\xi^2}\,(1-\kappa^2)^{\frac{1}{2}} \end{aligned}\right\} \tag{12.8}$$

Now by (10.18) we have $(1-\kappa^2)^{\frac{1}{2}} \doteqdot 2\pi\nu$ and so

$$\left.\begin{aligned} 1-p_+ &= 2\pi\nu(1-e^{-\frac{1}{2}\xi^2}) \\ 1-p_- &= 2\pi\nu\, e^{-\frac{1}{2}\xi^2}. \end{aligned}\right\} \tag{12.9}$$

Now substituting in (12.2) we get

$$\overline{H}_j = (2\pi\nu)^{-1}\, e^{\frac{1}{2}\xi^2}/(e^{\frac{1}{2}\xi^2}-1), \tag{12.10}$$

and similarly from (12.5)

$$\overline{G}_j = (2\pi\nu)^{-1}\, e^{\xi^2}/(e^{\frac{1}{2}\xi^2}-1). \tag{12.11}$$

These equations indicate that $\overline{H}$ and $\overline{G}$ are both inversely proportional to ν, as was also found in §§4 and 5. In fact if ν^2 is negligible, (4.5) and (5.5) can be written

$$\overline{G} = (2\pi)^{-\frac{1}{2}}\, e^{\frac{1}{2}\xi^2}/\nu\xi, \tag{12.12}$$

and

$$\overline{H} = (2\pi)^{-\frac{1}{2}}/\nu\xi \tag{12.13}$$

respectively.

TABLE 6. A COMPARISON OF THEORETICAL VALUES OF $\nu\overline{H}$ AND $\nu\overline{G}$

h^*	ξ	$\nu\overline{H}_j$ (12.10)	$\nu\overline{H}$ (12.13)	$\nu\overline{G}_j$ (12.11)	$\nu\overline{G}$ (12.12)
h_{mode}	1	0.404	0.399	0.667	0.658
h_{mean}	$(\frac{1}{2}\pi)^{\frac{1}{2}}$	0.293	0.318	0.642	0.698
$h_{\frac{1}{3}}$	2	0.184	0.199	1.360	1.474

The functional dependence on ξ in (12.10) and (12.11) is quite different from that in the two last equations. However, a numerical comparison is interesting. Table 6 shows the functions of ξ evaluated at three different levels: $h^* = h_{\text{mode}}$, h_{mean} and $h_{\frac{1}{3}}$ ($\xi = 1, \sqrt{(\frac{1}{2}\pi)}$ and 2). In every case the pairs of formulae, though analytically different, agree to within 10%. Hence over a certain range of ν and of ξ the two theories give quite similar results†.

† In fact, according to (9.10) we would expect the corresponding values of $\nu\overline{H}_j$ and $\nu\overline{H}$ to differ by a small amount of order 0.5 ν. For further discussion see Appendix B.

13. Discussion and conclusions

We have seen how two different approaches to the analysis of wave grouping can lead to almost identical results. Of these approaches, the first or Gaussian noise theory is more closely related to the wave spectrum, and is valid asymptotically as $\nu \to 0$. The second, or Markov, theory has been related roughly to the wave spectrum over an intermediate range of ν, which includes typical spectra of sea swell, and also suitably filtered spectra of wind waves.

As against this, the Gaussian theory is applicable strictly only to linear surface waves. When the waves become steep the harmonic components in a wave record are not independent, and the surface must become non-Gaussian. Markov theory, however, can still be applied, though its physical basis is not yet secure.

Whatever the relative merits of the two approaches, it appears that neither can be applied in a sensible way except to sufficiently narrow-band processes, or to data that have been filtered so as to eliminate both high and low frequencies. The same conclusion was also reached by Nolte & Hsu (1972, 1979) though the arguments for the tapered filter suggested in their 1979 paper do not appear to be conclusive. We have recommended a surface 'square-topped' filter with limits $0.5 f_p$ and $1.5 f_p$ which has two advantages:

(1) it leaves the peak frequency f_p unchanged;

(2) two successive applications of the filter have the same effect as only one.

Moreover, the chosen limits have been shown to give answers in agreement with a visual assessment of the group properties of the record.

This paper has confined attention to the essentially linear properties of wave groups. Some nonlinear statistical properties of wave groups deserve further attention, and studies directed towards this aspect are under way.

Appendix A. The swell spectrum (6.3)

To evaluate the moments of the spectrum $E(\sigma)$ of (6.3) we have from Erdelyi *et al.* (1954), equations (1.4.22) and (2.4.32), that when

$$f(x) = x^{-\frac{1}{2}} e^{-(\alpha x + \beta x^{-1})}, \tag{A 1}$$

then

$$\left.\begin{aligned} \int_0^\infty f(x) \cos xy \, dx &= \frac{\pi^{\frac{1}{2}}}{(\alpha^2+y^2)^{\frac{1}{2}}} e^{-2\beta^{\frac{1}{2}}u} \, (u \cos w - v \sin w), \\ \int_0^\infty f(x) \sin xy \, dx &= \frac{\pi^{\frac{1}{2}}}{(\alpha^2+y^2)^{\frac{1}{2}}} e^{-2\beta^{\frac{1}{2}}u} \, (u \sin w + v \cos w), \end{aligned}\right\} \tag{A 2}$$

where

$$\left.\begin{aligned} u &= \{\tfrac{1}{2}[(\alpha^2+y^2)^{\frac{1}{2}} + \alpha]\}^{\frac{1}{2}}, \\ v &= \{\tfrac{1}{2}[(\alpha^2+y^2)^{\frac{1}{2}} - \alpha]\}^{\frac{1}{2}}, \end{aligned}\right\} \tag{A 3}$$

and

$$w = 2\beta^{\frac{1}{2}} v. \tag{A 4}$$

Now letting $y \to 0$ in (A 3) we have

$$\left.\begin{aligned} u &= \alpha^{\frac{1}{2}}(1+y^2/8\alpha^2), \\ v &= y/2\alpha^{\frac{1}{2}}, \end{aligned}\right\} \tag{A 5}$$

to order y^2 and then from (A 2), on equating coefficients of 1, y and y^2,

$$\left.\begin{aligned} m_0^* &= (\pi^{\frac{1}{2}}/\alpha^{\frac{1}{2}})\,\mathrm{e}^{-2(\alpha\beta)^{\frac{1}{2}}}, \\ m_1^* &= (\pi^{\frac{1}{2}}/\alpha^{\frac{3}{2}})\,\mathrm{e}^{-2(\alpha\beta)^{\frac{1}{2}}}\,[\tfrac{1}{2}+(\alpha\beta)^{\frac{1}{2}}], \\ m_2^* &= (\pi^{\frac{1}{2}}/\alpha^{\frac{5}{2}})\,\mathrm{e}^{-2(\alpha\beta)^{\frac{1}{2}}}\,[\tfrac{3}{4}+\tfrac{3}{2}(\alpha\beta)^{\frac{1}{2}}+\alpha\beta]. \end{aligned}\right\} \tag{A 6}$$

Now writing

$$(\alpha\beta)^{\frac{1}{2}} = \tfrac{1}{2}n, \quad (\alpha/\beta)^{\frac{1}{2}}x = \sigma, \tag{A 7}$$

we have

$$\left.\begin{aligned} m_0 &= (\alpha/\beta)^{\frac{1}{2}}\,m_0^*, \\ \bar{\sigma} &= (\alpha/\beta)^{\frac{1}{2}}\,m_1^*/m_0^*, \\ \nu &= (\alpha/\beta)^{\frac{3}{2}}\,(m_2^*-m_1^{*2}/m_0^*). \end{aligned}\right\} \tag{A 8}$$

Substitution from (A 6) and (A 7) leads immediately to equations (6.4).

From (A 2) we have also, in the notation of § 10

$$\begin{aligned} X^2+Y^2 &= [\pi/(\alpha^2+y^2)]\,\mathrm{e}^{-4\beta^{\frac{1}{2}}u}(u^2+v^2) \\ &= [\pi/(\alpha^2+y^2)^{\frac{1}{2}}]\,\mathrm{e}^{-4(\alpha\beta)^{\frac{1}{2}}[\frac{1}{2}(1+y^2/\alpha^2)^{\frac{1}{2}}+\frac{1}{2}]}, \end{aligned} \tag{A 9}$$

and

$$\mu_0^2 = (\pi/\alpha)\,\mathrm{e}^{-4(\alpha\beta)^{\frac{1}{2}}}, \tag{A 10}$$

whence

$$\kappa^2 = (\alpha^2+y^2)^{-\frac{1}{2}}\,\mathrm{e}^{-4(\alpha\beta)^{\frac{1}{2}}\{[\frac{1}{2}(1+y^2/\alpha^2)^{\frac{1}{2}}+\frac{1}{2}]-1\}}. \tag{A 11}$$

On making the substitution (A 7) this becomes equation (11.4).

Appendix B. On the relation between discrete and continuous values of the group length

Suppose that discrete waves are identified by their crests, and that these are nearly equally spaced in regard to the time t. Take the wave period as unit of time.

In a continuous time interval of magnitude τ such that

$$i < \tau < i+1, \tag{B 1}$$

where i is a positive integer, there must be either i or $(i+1)$ wave crests. Assuming the crests are distributed uniformly in time, the probability of there being $(i+1)$ crests in the interval is $(\tau-i)$, and the probability of i crests is $(i+1-\tau)$. Hence we have

$$p(H_j) = \int_{j-1}^{j}(\tau-j+1)\,p(\tau)\,\mathrm{d}\tau+\int_{j}^{j+1}(j+1-\tau)\,p(\tau)\,\mathrm{d}\tau, \tag{B 2}$$

where $p(\tau)$ is the density of τ. Identifying τ with H, we see that H_j is the weighted mean of $p(H)$ by the triangular weighting function with base $(j-1, j+1)$ and height 1 (see figure 21).

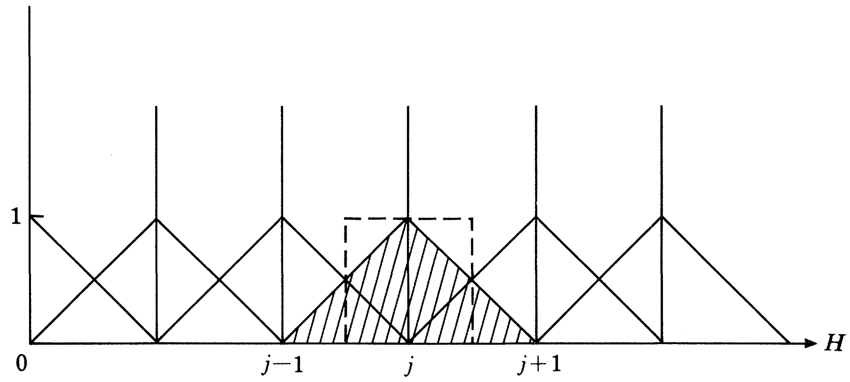

FIGURE 21. Form of the weighting function for $p(H)$ in the integral for H_j. Full-line: equation (B 2); broken line: equation (9.8).

Exceptionally when $j = 0$, only the right-hand half of the triangle is used. If $p(H_0)$ is set equal to zero, then $p(H_j), j > 0$ must be renormalized.

Now the rough approximation (9.8) amounts to replacing the triangular weighting function by the square with base $(j-\frac{1}{2}, j+\frac{1}{2})$ and height 1. Again, when $j = 0$ only the right-hand half of the square is used, and setting $p(H_0) = 0$ necessitates a renormalization.

This paper was begun while the author was visiting the California Technology Jet Propulsion Laboratory, Pasadena, in July 1983. He is indebted to Dr O. H. Shemdin, Dr V. Hsaio and Mr J. A. Ewing for kindly supplying the wave data discussed in §8. Useful discussions have been held with Mr D. J. T. Carter and Mr P. G. Challenor at I.O.S., Wormley. A first version of this paper was presented at the Whitecap Workshop held at University College, Galway, in September 1983.

REFERENCES

Abramowitz, M. & Stegun, I. A. (eds) 1965 *Handbook of mathematical functions.* New York: Dover.

Ahran, M. & Ezraty, R. 1978 Statistical relations between successive wave heights. *Oceanologia Acta* **1**, 151–158.

Burcharth, H. F. 1980 A comparison of nature waves and model waves, with special reference to wave grouping. *Proc. 17th Int. Conf. on Coastal Engng, Sydney*, pp. 2992–3009.

Donelan, M., Longuet-Higgins, M. S. & Turner, J. S. 1972 Periodicity in whitecaps. *Nature, Lond.* **239**, 449–451.

Erdelyi, A. (ed.) 1953 *Higher transcendental functions.* London: McGraw-Hill.

Erdelyi, A. (ed.) 1954 *Tables of integral transforms.* London: McGraw-Hill.

Erdelyi, A., Magnus, W., Oberhettinger, F. & Tricomi, F. G. 1954 *Tables of integral transforms*, vol. 1. New York: McGraw Hill. (391 pages.)

Ewing, J. A. 1973 Mean length of runs of high waves. *J. geophys. Res.* **78**, 1933–1936.

Favreau, R. R., Low, H. & Pfeffer, I. 1956 Evaluation of complex statistical functions by an analog computer. *Inst. Rad. Eng. Nat. Convention Record*, part 4, pp. 31–37.

Goda, Y. 1970 Numerical experiments on wave statistics with spectral simulation. *Rep. Port Harbour Res. Inst.* **9**, 3–75.

Goda, Y. 1976 On wave groups. *Proc. Conf. on Behaviour of Offshore Structures, Trondheim, Norway*, vol. 1, pp. 1–14. Trondheim: Norwegian Inst. of Tech.

Goda, Y. 1983 Analysis of wave grouping and spectra of long-travelled swell. *Rep. Port Harbour Res. Inst.* **22**, 3–41.

Hsaio, V. & Shemdin, O. H. 1983 Measurement of wind velocity and pressure with a wave follower during MARSEN. *J. geophys. Res.* **88**, 9841–9849.

Kimura, A. 1980 Statistical properties of random wave groups. *Proc. 17th Int. Conf. on Coastal Engng, Sydney*, pp. 2955–2973. New York: Am. Soc. Civ. Engrs.

Longuet-Higgins, M. S. 1952 The statistical distribution of the heights of sea waves. *J. mar. Res.* **11**, 245–266.
Longuet-Higgins, M. S. 1957 The statistical analysis of a random moving surface. *Phil. Trans. R. Soc. Lond.* A **249**, 321–387.
Longuet-Higgins, M. S. 1958 On the intervals between zeros of a random function. *Proc. R. Soc. Lond.* A **246**, 99–118.
Longuet-Higgins, M. S. 1962 The distribution of intervals between a stationary random function. *Phil. Trans. R. Soc. Lond.* A **254**, 557–599.
Longuet-Higgins, M. S. 1983 On the joint distribution of wave periods and amplitudes in a random wave field. *Proc. R. Soc. Lond.* A **389**, 241–258.
Middleton, D. 1960 *Statistical communication theory*. New York: McGraw-Hill.
Nolte, K. G. & Hsu, F. H. 1972 Statistics of ocean wave groups. *Proc. 4th Offshore Tech. Conf., Dallas, Texas*. Preprint no. 1688, pp. 139–146.
Nolte, K. G. & Hsu, F. H. 1979 Statistics of larger waves in a sea state. *Am. Soc. civ. Engrs, J. Waterway, Port, Coastal Ocean Div.* **105**, 389–404.
Ochi, M. K. 1982 Stochastic analysis and probabilistic prediction of random seas. *Adv. Hydrosci.* **13**, 217–375.
Pierson, W. J. (ed.) 1962 The directional spectrum of a wind generated sea as determined from data obtained by the Stereo Wave Observation Project. *N.Y. University Coll. Engrs*, Met. Pap. 2, no. 6.
Rice, S. O. 1944–1945 The mathematical analysis of random noise. *Bell Syst. Tech. J.* **23**, 282–332; **24**, 46–156.
Rice, S. O. 1958 Distribution of the duration of fades in radio transmission-gaussian noise model. *Bell Syst. Tech. J.* **37**, 581–635.
Rye, H. 1974 Wave group formation among storm waves. *Proc. 14th Int. Conf. on Coastal Engng*, pp. 164–183. New York: Am. Soc. Civ. Engrs.
Rye, H. & Lervik, E. 1981 Wave grouping studies by means of correlation techniques. *Norw. mar. Res.* **4**, 12–21.
Sawnhey, M. D. 1962 A study of ocean wave amplitudes in terms of the theory of runs and a Markhov chain process.
Siefert, W. 1974 Wave investigation in shallow water. *Proc. 14th Int. Conf. on Coastal Engng*, pp. 151–178. New York: Am. Soc. Civ. Engrs.
Uhlenbeck, G. E. 1943 Theory of random process. M.I.T. Radiation Lab. Rep. 454, October 1943.
Watson, G. N. 1958 *Theory of Bessel functions*. 2nd edn. Cambridge University Press. (804 pages.)
Wilson, J. R. & Baird, W. F. 1972 A discussion of some measured wave data. *Proc. 13th Int. Conf. on Coastal Engng*, pp. 113–130. New York: Am. Soc. Civ. Engrs.